R. & M. No. 3393

MINISTRY OF AVIATION

AERONAUTICAL RESEARCH COUNCIL
REPORTS AND MEMORANDA

Boundary-Layer Drag of Bi-Convex Wing Sections with Heat Transfer at Supersonic Speeds

By R. E. LUXTON and A. D. YOUNG
Queen Mary College, London

LONDON: HER MAJESTY'S STATIONERY OFFICE
1965
PRICE 18*s.* 0*d.* NET

Boundary-Layer Drag of Bi-Convex Wing Sections with Heat Transfer at Supersonic Speeds

By R. E. LUXTON* and A. D. YOUNG
Queen Mary College, London

Reports and Memoranda No. 3393†
March, 1964

Summary.

Previously published methods for the calculation of the skin friction and growth of compressible laminar and turbulent boundary layers in the presence of heat transfer (Refs. 1 and 2) are applied to bi-convex wings of 5% thickness at Mach numbers of 1·5, 2·5 and 5·0, and Reynolds numbers of 10^6, 10^7 and 10^8 for a range of transition points and a range of heat-transfer conditions. Similar calculations are also made for a flat plate at zero incidence for the same ranges of Reynolds number and Mach number. It is shown that the effect of rearward movement of transition is reduced by increase in Mach number, by reduction in Reynolds number and by increase in the wall to recovery temperature ratio. These results are explained in terms of the relative sensitivities of the laminar and turbulent boundary layers to these parameters. Some discussion is offered of the effects on skin friction of the interaction between the boundary layer and the external flow and also the effects of small changes in the Prandtl number and viscosity-temperature index are considered.

It is shown that in general cooling of the surface causes an increase in drag for all transition points except those very close to the trailing edge.

It is concluded that if wing surfaces are cooled to avoid the otherwise serious effects of aerodynamic heating at high speeds then with increase in Mach number it becomes increasingly desirable for the boundary layer to be kept laminar to very near the trailing edge.

LIST OF CONTENTS

* Now at the Department of Mechanical Engineering, University of Sydney.

† Replaces A.R.C. 25 685.

LIST OF CONTENTS—*continued*

---

1. *Introduction.*

The flow over bi-convex wings with zero heat transfer at the surface has been considered in Refs. 5, 6, 7 and 8. The present work is essentially an extension of this work to investigate the effects of heat transfer at the surface. The projected development of supersonic aircraft has made these effects of particular practical importance.

In Refs. 1 and 2 methods have been presented for the calculation of the growth of laminar and turbulent boundary layers, respectively, on non-insulated walls in a compressible flow. In this paper, these methods are applied to the flow over a 5% thick bi-convex wing and over a flat plate at zero incidence.

As in the previous work the process of determining the boundary-layer drag has involved following first the development of the boundary layer in the laminar and the turbulent states for a specified transition position and the inviscid-flow pressure distribution and then a first-order assessment of the effect of the boundary layer on the surface pressure distribution is obtained. Thus both the skin-friction drag and the boundary-layer pressure drag are determined. Shock-wave/boundary-layer interaction effects at the trailing edge are assumed to be negligible for the cases considered.

It may be noted, however, that the pressure change from inviscid flow produced by the boundary layer is not the sole effect of the interaction between the boundary layer and the external flow. A secondary but by no means negligible effect (*see* Ref. 6) is that the modification of the pressure

distribution alters the skin-friction distribution from that found from the initial assumption of an inviscid pressure distribution. This effect has been considered in Ref. 6 for the case of zero heat transfer and on the basis of that work an assessment of the corresponding effect with heat transfer is presented here (*see* Section 7).

It must here be remarked that the 'mean enthalpy' approach used by Spence[2] for the turbulent boundary layer differs from that developed by Young[5] and used for the zero heat-transfer calculations of Refs. 6 and 8. The difference lies essentially in the assumptions used to extrapolate from incompressible to compressible flow for the basic case of the flat plate at zero incidence. In both cases the numerical results for skin friction are in good agreement for the ranges of Mach number and Reynolds number of the available experimental data used to check the method of Ref. 5 ($R \simeq 10^7$, $M < 4{\cdot}5$). However, the assumptions are such that Young's method is more sensitive to variations of Reynolds number when it is low, particularly at high Mach numbers, than is Spence's method[13]. Thus at the lowest Reynolds number and highest Mach number here considered (10^6 and 5, respectively) the difference between the two methods is considerable (about 50 per cent) although the difference rapidly becomes very small with increase of Reynolds number or decrease of Mach number. A generalisation of Young's method to the case of non-zero heat transfer was in fact developed at an early stage in this work but it was subsequently felt that the weight of current thought of workers in this field as well as more recent experimental evidence was on the whole in favour of the mean enthalpy concept. For this reason Spence's method was finally adopted here.

It must be noted, however, that as yet the experimental evidence on skin friction for cases of marked heat transfer and supersonic speeds is still too sparse to offer convincing support or otherwise for any of the many available theories. The essentially empirical nature of theories of the turbulent boundary layer must not be forgotten and the need for more experimental data of adequate reliability cannot be too strongly stressed. However, results presented here can be regarded as plausible in the light of current data and thinking and past experience.

The ranges of the main variables covered in the calculations for the bi-convex wing presented here are,

$$\text{Mach number } M_\infty = 1{\cdot}5,\ 2{\cdot}5,\ 5{\cdot}0,$$

$$\text{Reynolds number } R_\infty = 10^6,\ 10^7,\ 10^8,$$

Transition Point $x_T/c = 0{\cdot}05,\ 0{\cdot}25,\ 0{\cdot}50,\ 0{\cdot}75,\ 1{\cdot}00$ and Heat-Transfer Parameter $S_w = T_w/T_r - 1 = -0{\cdot}8,\ -0{\cdot}4,\ 0,\ +0{\cdot}4$. The suffix $_\infty$ refers to conditions in the undisturbed free stream ahead of the leading edge. We note that when $S_w > 0$, heat is passing from the wall to the fluid and when $S_w < 0$, heat is passing from the fluid to the wall.

In the case of the flat plate the calculations are for fully laminar and fully turbulent flow over the same ranges of Mach number and Reynolds number as for the bi-convex wing.

The values of the Prandtl number σ and the temperature-viscosity relationship index ω have generally been taken as $0{\cdot}725$ and $0{\cdot}89$ respectively. However, from Fig. 1 it may be seen that a value of $\omega = 0{\cdot}89$ is reasonable when the ambient temperature is between about -110 and $+140$°C, but as the temperature rises the appropriate value of ω falls. For example, with zero heat transfer, the surface of a wing in flight at $M_\infty = 5{\cdot}0$ and 50,000 feet could reach a temperature of about 850 →900°C and the value of ω appropriate to this temperature is about $0{\cdot}65$. It was felt therefore that some indication of the effects of changes in ω and σ should be presented and this is done in Section 8.

The calculations have been programmed for the University of London Computer Unit 'Mercury' Computer. Unless otherwise stated the drag coefficients quoted apply to one surface and should be doubled for the complete wing.

2. *Summary of Calculation Methods.*

The methods of calculation of the skin friction in the laminar and turbulent boundary layers are those presented in Refs. 1 and 2 respectively. For convenience the main formulae are summarised here.

2.1. *Laminar Boundary Layer.*

A transformed co-ordinate normal to the wall is defined by

$$Y = \int_0^y \frac{\mu_1}{\mu}\, dy, \tag{1}$$

where μ is the coefficient of viscosity, taken to be proportional to T^ω. The velocity distribution is assumed to be a quartic in Y, and the thickness of the transformed boundary layer is δ_1 where δ_1 is the value of Y corresponding to the value of y defining the edge of the physical boundary layer. The functions $H = \delta^*/\theta$ and $f = \delta_1/\theta$, where δ^* and θ are respectively the displacement and momentum thicknesses of the boundary layer, are assumed to be functions of local Mach number, local wall to free-stream temperature ratio, and local pressure gradient. In addition f is a function of ω and σ where σ is the Prandtl number.

The value of H is given at each point on the surface by

$$H = [2{\cdot}59\,(1+S_w) + k_2\Lambda]\left(1 + \frac{\gamma-1}{2} M_1^2\sigma^{1/2}\right) + \frac{\gamma-1}{2} M_1^2, \tag{2}$$

where Λ is a Pohlhausen-type pressure-gradient parameter defined by

$$\Lambda = \frac{du}{dx}\delta_1^2\rho_1\frac{\mu_w}{\mu_1^2}, \tag{3}$$

M_1 is the local free-stream Mach number,

k_2 is a correction factor defined and evaluated in Ref. 1,

and S_w is defined by

$$S_w = \frac{T_w}{T_r} - 1, \tag{4}$$

where T_w and T_r are the wall and recovery temperatures, respectively,

Similarly, the local value of f is given by

$$f = f_z(1+k_1\Lambda) \tag{5}$$

where

$$f_z = 9{\cdot}072\left[0{\cdot}45 + 0{\cdot}55\,\frac{T_w}{T_1} + 0{\cdot}09\,(\gamma-1)M_1^2\sigma^{1/2}\right]^{1-\omega}, \tag{6}$$

and k_1 is a correction factor defined and evaluated in Ref. 1†.

---

† In Ref. 1 f_z was denoted $f_{f.p.}$ since it is the value of f for zero pressure gradient appropriate to a flat plate at zero incidence.

For the solution of the momentum equation the boundary layer is considered in steps of suitable magnitude for each of which H and f are assumed constant and equal to their values at the beginning of the step. Thus, for the step between x_n and x_{n+1} we obtain in non-dimensional form

$$\left[\left(\frac{\rho_1}{\rho_a}\right)^2\left(\frac{\theta}{c}\right)^2 R_a\right]_{n+1} - \left[\left(\frac{\rho_1}{\rho_a}\right)^2\left(\frac{\theta}{c}\right)^2 R_a\right]_n \frac{\left[\left(\frac{u_1}{u_a}\right)^{g_n}\right]_n}{\left[\left(\frac{u_1}{u_a}\right)^{g_n}\right]_{n+1}}$$

$$= \frac{4}{\left[\left(\frac{u_1}{u_a}\right)^{g_n}\right]_{n+1}} \int_{x_n/c}^{x_{n+1}/c} \frac{\left(\frac{\rho_1}{\rho_a}\right)\left(\frac{\mu_1}{\mu_a}\right)\left(\frac{u_1}{u_a}\right)^{(g_n-1)}}{f_n} d\frac{x}{c} \tag{7}$$

where n, $n+1$ refer to values at x_n, x_{n+1} along the surface,

c is the chord length,

R_a is the Reynolds number defined by $R_a = \rho_a \mu_a c/\mu_a$,

suffix a refers to suitable reference conditions such as conditions aft of the leading-edge shock, and g_n is a function of H_n, f_n and μ_w/μ_1, defined by

$$g_n = 2\left[(H_n+2) - \frac{f_n}{6}\frac{\mu_w}{\mu_1}\right] \tag{8}$$

and is taken as constant over the interval x_n to x_{n+1}.

The skin-friction coefficient based on leading-edge reference condition c_{fa} then satisfies

$$c_{fa}\sqrt{R_x} = \frac{2\tau_w}{\rho_a {u_a}^2}\sqrt{\frac{\rho_a u_a x}{\mu_a}} = \frac{\frac{\mu_1}{\mu_a}(12+\Lambda)\frac{u_1}{u_a}\left(\frac{x}{c}\right)^{1/2}}{3f\frac{\theta}{c}\sqrt{R_a}}. \tag{9}$$

Values of the displacement thickness δ^* may be found from the values of θ and H.

Simplified versions of the above 'complete' method are described in Ref. 1.

2.2. *Turbulent Boundary Layer.*

Spence, Ref. 2, showed from an analysis of experimental data that with good approximation the turbulent velocity profile for a flat plate at zero incidence could be represented by

$$\frac{u}{u_1} = \Phi(\eta/\Delta), \text{ say,} \tag{10}$$

where

$$\eta = \int_0^y \frac{\rho}{\rho_1} dy \qquad \text{and} \qquad \Delta = \int_0^\delta \frac{\rho}{\rho_1} dy, \tag{11}$$

and Φ was a function of η/Δ, only, independent of Mach number (at least up to $M = 8$) and wall temperature. He also demonstrated the validity of a quadratic relationship between the temperature and velocity in the boundary layer and hence deduced that

$$H = \frac{T_w}{T_1} H_{i,0} + \frac{T_r}{T_1} - 1 \tag{12}$$

where $H_{i,0}$ is the value of H in incompressible flow with zero heat transfer.

He then used this expression for H and a Stewartson-Illingworth type of transformation of the momentum equation for the general case of an external pressure gradient and thereby reduced the left-hand side of the equation to the simplicity of its incompressible-flow form. The equation was then solved by making use on the right-hand side of a 'flat plate' relation between momentum thickness and skin friction derived from Eckert's mean enthalpy concept.

In the present calculations, the Sommer and Short (Ref. 3) mean temperature has been used as it gives slightly better agreement with available experimental data (Refs. 3 and 4) than does the Eckert relationship. Sommer and Short's temperature is, for $\sigma = 0{\cdot}725$, T_{mt} where

$$\left.\begin{aligned} \frac{T_{mt}}{T_1} &= 0{\cdot}55 + 0{\cdot}035M_1^2 + 0{\cdot}45\,(1+S_w)\,\frac{T_r}{T_1} \\ &= 0{\cdot}55 + 0{\cdot}195\left(\frac{T_r}{T_1} - 1\right) + 0{\cdot}45\,\frac{T_w}{T_1}, \quad \text{with} \quad \sigma = 0{\cdot}725. \end{aligned}\right\} \tag{13}$$

Here, the value of T_r for the turbulent boundary layer is taken to be

$$T_r = T_1\left[1 + \frac{(\gamma-1)}{2}\,M_1^2\sigma^{1/3}\right].$$

The integrated momentum equation with $\omega = 0{\cdot}89$ and a velocity profile of the form

$$\frac{u}{u_1} = \left(\frac{\eta}{\Delta}\right)^{1/9} \tag{14}$$

then becomes

$$\left(\frac{\theta}{c}\right)^{1{\cdot}2} M_1^{B+0{\cdot}2}\,G(M_1) = 0{\cdot}0106\,R_{c0}^{-0{\cdot}2}\int_{xT/c}^{x/c} M_1^B F(M_1)d\left(\frac{x}{L}\right) + K_T \tag{15}$$

where

$$R_{c0} = \frac{a_0 c}{\nu_0} = R_a\,\frac{[1 + 0{\cdot}2M_a^2]^{3-\omega}}{M_a},$$

K_T is the value of the left-hand side at the transition point at which θ is assumed continuous, and $G(M_1)$, $F(M_1)$ and B are given in the following table.

	Zero Heat Transfer	Constant Temperature Wall
B	4	$1{\cdot}8\,\frac{T_w}{T_0} + 2{\cdot}2$
$F(M_1)$	$\left(\frac{T_1}{T_0}\right)^{3{\cdot}331}\left(\frac{T_{mt}}{T_1}\right)^{-0{\cdot}822}$	$\left(\frac{T_1}{T_0}\right)^{3{\cdot}239}\left(\frac{T_{mt}}{T_1}\right)^{-0{\cdot}822}$
$G(M_1)$	$\left(\frac{T_1}{T_0}\right)^{3{\cdot}753}$	$\left(\frac{T_1}{T_0}\right)^{3{\cdot}661}$
$\frac{T_{mt}}{T_1}$	$1 + 0{\cdot}1158M_1^2$	$0{\cdot}55 + 0{\cdot}035M_1^2 + 0{\cdot}45T_w/T_1$
$\frac{T_1}{T_0}$	$(1+0{\cdot}2M_1^2)^{-1}$	$(1+0{\cdot}2M_1^2)^{-1}$

The skin-friction coefficient is then found by substituting the value of θ obtained from (15) into

$$(c_f)_{\text{local}} = \frac{2\tau_w}{\rho_1 u_1^2} = \frac{0{\cdot}0176\,[1 + 0{\cdot}2M_a^2]^{1/10}}{M_a^{1/5}} \left[\frac{u_a}{u_1}\right]^{1/5} \left[\frac{T_{mt}}{T_1}\right]^{\omega/5-1} \left[\frac{T_1}{T_0}\right]^{\omega/5-1/2} \left[\frac{\theta}{c} R_{c0}\right]^{-1/5} \tag{16}$$

and

$$c_{fa} = \left(\frac{u_1}{u_a}\right)^2 \left(\frac{T_1}{T_a}\right)^{2{\cdot}5} (c_f)_{\text{local}}. \tag{17}$$

2.3. *Boundary-Layer Pressure Drag.*

The method used for the calculation of the boundary-layer pressure drag is that given in Ref. 5. If the flow outside the boundary layer is regarded as a simple wave flow, then, to a first order, the change in local pressure due to the boundary layer is shown in Ref. 5 to be

$$\Delta p = \frac{\rho_1 u_1^2}{\sqrt{(M_1^2 - 1)}} \frac{d\delta^*}{dx}. \tag{18}$$

Equation (18) may be integrated to give the boundary-layer pressure drag ΔC_{Dp1} provided some plausible assumption is made regarding the value of $d\delta^*/dx$ as $x \to 0$. In the present calculations it has been assumed that the value of $d\delta^*/dx$ in the range $0 \leqslant x/c \leqslant 0{\cdot}05$ is constant and equal to the value of $d\delta^*/dx$ at $x = 0{\cdot}05$. In Appendix II of Ref. 6, is presented a strong argument in support of such an assumption†.

In Ref. 8 it is also postulated that the discontinuity in δ^* at the transition point, caused by assuming θ continuous there, contributes to the boundary-layer pressure drag. This component is given by

$$\Delta C_{DpT} = \pm \frac{2\rho_1 u_1^2}{\rho_\infty u_\infty^2} \frac{dy_s}{dx} \frac{\delta_{lT}^* - \delta_{tT}^*}{c} \frac{1}{\sqrt{(M_{1T}^2 - 1)}} \tag{19}$$

where dy_s/dx is the surface slope at the transition point, and δ_{lT}^* and δ_{tT}^* are the displacement thicknesses at the transition point for the turbulent and the laminar boundary layers. The '+' sign refers to the upper surface and the '−' sign refers to the lower surface of the wing. In general δ_{tT}^* is smaller than δ_{lT}^* since the value of H_t for a turbulent boundary layer is usually smaller than H_l for a laminar boundary layer. Under these conditions we may expect ΔC_{DpT} to be negative on the forward part of the wing where dy_s/dx is positive, for the upper surface, and to be positive over the rear of the wing where dy_s/dx is negative. For cases involving high rates of cooling, however, the values of H in the laminar and turbulent layers may become more nearly equal and in some cases H_t may become greater than H_l. In this case the signs of ΔC_{DpT} on the forward and rear portions of the wing would be the opposite of those quoted above. It should be noted that allowance has also been made for ΔC_{DpT} in the case of transition at the trailing edge. If the boundary layer was laminar to the trailing edge, then it is likely for the bi-convex wing that the trailing-edge shock wave would cause separation of the boundary layer for some distance upstream of the trailing edge, with consequent large changes in the drag. With the boundary layer turbulent no significant region of separation need be expected (Ref. 11). The case $x_T/c = 1$ is, therefore, taken as the limiting case for diminishing amounts of turbulent flow on the wing and as such it is assumed that there is no shock-induced separation.

† In Ref. 6 $d\delta^*/dx$ is taken as constant in the range $0 \leqslant x/c \leqslant 0{\cdot}04$ but the arguments presented there indicate that no significant error can arise if the range $0 \leqslant x/c \leqslant 0{\cdot}05$ is taken.

In non-dimensional form the total boundary-layer pressure-drag coefficient becomes, for the upper surface of a bi-convex wing,

$$\Delta C_{Dp} = \Delta C_{Dp1} + \Delta C_{DpT} = \frac{2\rho_a {u_a}^2}{\rho_\infty {u_\infty}^2} \int_0^{x_T/c} \frac{\rho_1 {u_1}^2}{\rho_a {u_a}^2} \frac{\sin\beta}{\sqrt{({M_1}^2-1)}} \frac{d\left(\frac{\delta_t^*}{c}\right)}{d\left(\frac{x}{c}\right)} d\left(\frac{x}{c}\right) +$$

$$+ \frac{2\rho_a {u_a}^2}{\rho_\infty {u_\infty}^2} \int_{x_T/c}^1 \frac{\rho_1 {u_1}^2}{\rho_a {u_a}^2} \frac{\sin\beta}{\sqrt{({M_1}^2-1)}} \frac{d\left(\frac{\delta^*_t}{c}\right)}{d\left(\frac{x}{c}\right)} d\left(\frac{x}{c}\right) + \frac{2\rho_a {u_a}^2}{\rho_\infty {u_\infty}^2} \frac{\rho_1 {u_1}^2}{\rho_a {u_a}^2} \frac{\sin\beta_T}{\sqrt{({M_{1T}}^2-1)}} \left[\frac{\delta_{tT}{}^*}{c} - \frac{\delta_{tT}{}^*}{c}\right] \quad (20)$$

Suffix T denotes values at the transition point, β is the surface slope relative to the x axis.

3. *Results and Discussion for Fully Laminar Flow on the Bi-Convex Aerofoil.*

The fact demonstrated in Ref. 1, that when the boundary layer is laminar and the pressure gradient is favourable cooling tends to reduce the skin friction, makes the prospect of wings with fully laminar flow particularly attractive for high-speed flight. It is therefore of some interest to see how the calculated distributions of the major boundary-layer characteristics vary with heat transfer and Mach number with the boundary layers fully laminar on the 5% thick bi-convex section. The chordwise skin-friction distributions (based on conditions aft of the leading-edge shock wave) are presented in Figs. 2, 3 and 4 for the three Mach numbers considered. These results display the same reduction of skin friction with cooling as the simple case with a favourable pressure gradient considered in Ref. 1. It will be noted that with increase of Mach number the forward part of the wing contributes an increasing part of the total skin-friction drag. This is discussed in Ref. 6 where the effect was explained as due to the related changes of the chordwise distribution of the dynamic pressure outside the boundary layer ($\rho_1 {u_1}^2/\rho_a {u_a}^2$) as well as of the distribution of local Mach number (M_1) there. Typically at supersonic main-stream Mach numbers the local Mach number increases whilst the dynamic pressure decreases from the leading edge to the trailing edge and these effects are enhanced by increase of main-stream Mach number (*see* Figs. 19 and 21 of Ref. 6). Since the skin friction increases with increase of dynamic pressure and reduction of local Mach number the calculated trends are readily explained.

The dotted curves on each of Figs. 2, 3 and 4 show the results for the wall temperatures equal to the ambient temperatures ($T_w = T_a$), a condition that approximates to that likely to be aimed at in practice.

The distributions of momentum thickness θ/c and the form factor $H = \delta^*/\theta$ for the fully laminar boundary layer are plotted in Figs. 5, 6 and 7 for $M = 1{\cdot}5$, $2{\cdot}5$ and $5{\cdot}0$ respectively. It is interesting to note that the rate of growth of momentum thickness $d\theta/dx$ is considerably greater at $M_\infty = 5{\cdot}0$ than at the lower Mach numbers. Further, cooling tends to increase this rate of growth, the increase being greatest at the highest Mach number. If it were not for the effect of the pressure gradient as well as that of the associated distribution of $\rho_1 {u_1}^2/\rho_a {u_a}^2$, one would expect the skin-friction coefficient to reflect the behaviour of $d\theta/dx$ and to increase with cooling and with increasing Mach number. The reverse is in fact the case as is shown in Figs. 2, 3 and 4. The essential physical cause for the pressure-gradient effect with cooling is discussed fully in Ref. 1 but the argument is briefly summarised again in Section 5.

The form factor H is reduced by cooling the surface at a given Mach number, but is increased considerably as the Mach number is increased at a given value of S_w. The reduction in the form factor with cooling at a constant Mach number is partly due to the increase of θ and partly due to a reduction in the displacement thickness δ^*. For example, at $M_\infty = 5{\cdot}0$, $[(\delta^*/c)\sqrt{R_a}]_{x=c}$ is $18{\cdot}7$ for zero heat transfer but is only $7{\cdot}3$ when $S_w = -0{\cdot}8$. From this we may expect a considerable reduction with cooling in the effect associated with the displacement thickness of the boundary layer on the external pressure distribution, and hence a reduction in the boundary-layer pressure drag. It may be noted that the distribution of H is very nearly constant along the chord in all cases save those for a heated wall and for zero heat transfer at $M_\infty = 5{\cdot}0$. This offers some 'a posteriori' justification in the case of favourable pressure gradients for the assumption that H is constant made in the 'first simple' method of Ref. 1.

The overall skin-friction results for a fully-laminar-flow aerofoil are summarised in Fig. 8 in which $C_{F\infty}\sqrt{R_\infty}$ is plotted as a function of M_∞ for different values of S_w. The skin friction appears to reach a minimum value at a Mach number M_∞ of between $3{\cdot}0$ and $3{\cdot}5$, depending on the heat-transfer rate. This minimum is less pronounced when the cooling rate is high. The factors which determine where the minimum value occurs and its magnitude are very complex. They can only be disentangled by a detailed consideration of the effects of the changes of the pressure and Mach number distributions along the wing surface with changes in main-stream Mach number.

4. *Flat Plate at Zero Incidence* (*Laminar and Turbulent Boundary Layers*†).

The calculated results of overall skin-friction coefficient for the flat plate at zero incidence with fully laminar and fully turbulent boundary layers are given in Table 1 and are also shown in Fig. 9.

The large effects of both wall heating and increase of Mach number on the skin friction when the boundary layer is turbulent and the corresponding small effects when the boundary layer is laminar are immediately evident.

The small effects in the case of the laminar boundary layer for the value of ω assumed are reflected in the formula (Ref. 9)

$$C_f\sqrt{R_x} = 0{\cdot}664\left[0{\cdot}45 + 0{\cdot}55\,\frac{T_w}{T_1} + 0{\cdot}09\,(\gamma-1)M_1^2\sigma^{1/2}\right]^{-(1-\omega)/2} \tag{21}$$

from which we can deduce that

$$C_{F\infty}\sqrt{R_\infty} = 1{\cdot}328\left(\frac{T_{ml}}{T_1}\right)^{-(1-\omega)/2} \tag{22}$$

where

$$\left.\begin{aligned} T_{ml} &= T_1\left[0{\cdot}45 + 0{\cdot}55\,\frac{T_w}{T_1} + 0{\cdot}09\,(\gamma-1)M_1^2\sigma^{1/2}\right] \\ \text{or} \quad T_{ml} &= 0{\cdot}45\,T_1 + 0{\cdot}55\,T_w + 0{\cdot}18\,(T_r - T_1), \end{aligned}\right\} \tag{23}$$

i.e. T_{ml} is a mean temperature for the laminar boundary layer which is in fact not very different from the accepted mean temperature for the turbulent boundary layer {*see* equation (13)}. We see that as long as ω is near unity the effects of changes of T_w and M_1 on the skin-friction coefficients must be small. In effect, any changes in density and viscosity in the boundary layer near the wall

† It should be noted that where overall values of skin friction and boundary-layer drag are presented in this paper they refer to one surface only, for a complete wing therefore these values should be multiplied by a factor 2.

due to changes of wall temperature or Mach number are largely compensated for, as far as the skin friction is concerned, by a corresponding change in velocity distribution to keep the skin friction nearly constant (when $\omega = 1 \cdot 0$, this compensation is exact).

However, with the boundary layer turbulent Spence's method leads to the formula

$$C_{F\infty} R_{\infty}^{1/6} = 0 \cdot 0450 \, (T_{mt}/T_1)^{-(5-\omega)/6} \tag{24}$$

where T_{mt} is given by equation (13).

In this case the exponent of (T_{mt}/T_1) is about $-2/3$ and so $C_{F\infty}$ is much more sensitive to changes of T_{mt} with changes of T_w and M_1. This can be explained physically by arguing that an increase of wall temperature, due either to an increase of S_w or Mach number, will reduce the density and increase the viscosity of the air near the surface. The reduction of density will tend to reduce the skin friction and the increase of viscosity will tend to increase it, but in the turbulent boundary layer the latter effect is much less important as manifest in the relative insensitivity of the skin friction to changes of Reynolds number. Unlike the case of the laminar boundary layer the velocity profile of the turbulent boundary layer is in the light of experimental evidence in large part relatively insensitive to changes of Mach number and wall temperature and so this compensating mechanism of the laminar boundary layer is less evident. The net result is a marked dependence of the skin friction in the turbulent boundary layer on wall temperature and Mach number and this dependence can be regarded as determined very largely by the corresponding density changes near the wall.

5. *The Combined Effects of Heat Transfer and Pressure Gradient.*

In Ref. 1 it is shown that, with the boundary layer laminar, if the wall temperature is reduced in the presence of a favourable (negative) pressure gradient then the skin friction is reduced whilst in the presence of an adverse gradient the skin friction is increased by wall cooling. Converse effects occur when the wall is heated. This was explained simply by the argument that with wall cooling the density of the air is increased near the wall and hence it responds less readily to the external pressure gradient. With the gradient favourable the air is then less readily accelerated and so the skin friction is reduced by the wall cooling, whilst with the gradient adverse the deceleration of the air is reduced by the cooling and so the skin friction is increased. At the heart of this argument lies the fact that the velocity distribution in the laminar boundary layer is very sensitive to external pressure gradients.

However, with the boundary layer turbulent, experimental evidence at low Mach numbers shows that the inner part of the layer is extremely insensitive to other than strong adverse pressure gradients. Indeed, for small adverse pressure gradients and for favourable pressure gradients the velocity profile as a whole is fairly insensitive to the pressure gradients*. It is argued that this is because of the dominance of the macroscopic momentum and energy transfer processes by the turbulent eddies which impose a measure of flow similarity on the inner part of the boundary layer largely independent of the pressure gradient. There is little experimental evidence on the sensitivity or otherwise of turbulent boundary layers to pressure gradients at high Mach numbers and it is undoubtedly desirable that such experiments should be made. However, in the absence of such experiments it is reasonable to assume that the same powerful mechanism will operate at high Mach numbers as at low to ensure an inner region in the boundary layer for which the velocity profile will be relatively

* For a discussion of this *see* Ref. 10, Ch. 6.

insensitive to pressure gradients and this inner region can be expected to be large with favourable pressure gradients. This assumption is indeed implicit in Spence's method used here as it is in almost all other methods that have been devised for dealing with the turbulent boundary layer in compressible flow for cases where the pressure gradients are not so large and adverse as to make flow separation imminent. From this assumption it then follows that the dominant effects of wall cooling or heating on skin friction will be simply and directly those associated with the corresponding density changes near the wall and these will be little affected by any moderate pressure gradient. Thus in such cases wall cooling will be accompanied by an increase of skin friction and conversely wall heating will be accompanied by a decrease of skin friction.

To illustrate this Fig. 10 shows the calculated skin-friction distributions along the length of a plate subject to an adverse pressure gradient with a fully laminar boundary layer and with transition to a turbulent state starting very close to the leading edge. A strongly cooled wall ($S_w = -0{\cdot}731$) and a wall with zero heat transfer is considered in each case. In the case of the laminar boundary layer, separation occurs relatively early without cooling and as is to be expected the effect of wall cooling is to cause a marked increase of skin friction and a considerable delay in separation. Here both the direct density effect as well as its coupling with the pressure gradient combine to produce a very considerable change due to cooling. In the case of the turbulent boundary layer we again get an increase of skin friction due to cooling as is to be expected from the above argument although it is relatively less spectacular than with the laminar boundary layer. The general increase of the skin friction with distance along the surface with the boundary layer turbulent is due to the associated increase of dynamic pressure outside the boundary layer coupled with the insensitivity of the velocity profile to the pressure gradient. On the other hand in Fig. 13 are presented the overall values of the skin-friction coefficients for the 5% thick bi-convex wing section plotted as functions of Mach number for various values of the heat-transfer parameter S_w and for fully turbulent and fully laminar boundary layers. In this case the pressure gradient is favourable. Here again we see the marked increase of skin friction with wall cooling or with decrease of Mach number for the turbulent boundary layer. For the laminar boundary layer, however, the effects of the favourable pressure gradient (small as it is) is quite enough to reverse the direct density effect on skin friction so that wall cooling produces a reduction of skin friction.

To summarise this section and the preceding one, we see that in the absence of any pressure gradient the skin friction with the boundary layer laminar is much less sensitive to changes of wall temperature and Mach number than is the skin friction with the boundary layer turbulent. The latter, however, is much less sensitive than the former to the effects of an external pressure gradient. We must however again emphasise that our knowledge of the turbulent boundary layer at high Mach numbers and in the presence of pressure gradients and heat transfer is inadequate to provide complete confirmation of the theory used, although it is most unlikely that the broad results of this theory are seriously misleading for the ranges of the main variables considered here.

6. *Results for the Bi-Convex Wing and Discussion.*

The overall results for all transition points considered are presented in Table 2 and in Figs. 13, 14, 15, 16 ($C_{F\infty}$), 17, 18, 19 (ΔC_{Dp}), 20, 21 and 22 (C_{DB}).

6.1. *Skin Friction and Momentum Thickness.*

An example of the chordwise distribution of skin friction for various transition points is given in Fig. 11 for $M_\infty = 2{\cdot}5$ and $R_\infty = 10^7$ for $S_w = 0$ (zero heat transfer) and $S_w = -0{\cdot}8$

($T_w \approx 0{\cdot}47 T_\infty$). The large increase in turbulent skin friction due to cooling is in marked contrast to the corresponding small decrease in laminar skin friction. This is in accordance with the general trends discussed in the previous section.

An illustration of the growth of momentum thickness for different transition positions, cooling rates and Reynolds numbers, is given in Fig. 12 for $M_\infty = 1{\cdot}5$. The chordwise rate of growth of θ increases with cooling and with decrease in Reynolds number. In the turbulent boundary layer this is reflected in an increase in the skin-friction coefficient with increase in the cooling rate, as noted above, and with reduction of the Reynolds number. In the laminar boundary layer, however, it has already been remarked in Sections 3 and 5 that the combination of favourable pressure gradient and cooling is sufficient to cause a reduction in skin friction.

The overall skin-friction coefficients for the cases of fully turbulent and fully laminar flow are summarised for $R_\infty = 10^7$ in Fig. 13. We note that the difference between the skin friction for laminar and turbulent flow is reduced as the Mach number is increased. This follows from the greater sensitivity of the turbulent boundary layer to changes of Mach number. The overall skin friction with a fully turbulent boundary layer for the case $T_w = T_\infty$, where T_∞ is the temperature of the undisturbed free stream, is plotted in Fig. 13 to illustrate a possible practical case.

As in the case of zero heat transfer (Ref. 7) the effect on the skin friction of rearward movement of transition is reduced with increase in Mach number and with decrease in Reynolds number, Figs. 14, 15 and 16. It has already been noted that the turbulent boundary layer is much more sensitive to changes in Mach number than is the laminar boundary layer, the former is also less sensitive to changes in Reynolds number than the latter. We have also noted the local Mach number increases and the product $\rho_1 u_1^2$ decreases (except for M_∞ less than about $1{\cdot}5$) with distance downstream from the leading edge of the wing and these effects increase with increase of main-stream Mach number. Thus, as the Mach number is increased and the Reynolds number reduced, the laminar skin friction on the forward portion of the wing contributes an increasing part of the overall skin friction and movement of the transition point has a decreasing effect on the overall skin friction. However, since cooling enhances the turbulent boundary-layer skin friction and reduces slightly the laminar boundary-layer skin friction, it tends to increase the magnitude of the negative slope of the skin-friction drag against rearward movement of transition position. Heating, of course, has the opposite effect and in the somewhat unlikely case of a heated wing at $M_\infty = 5{\cdot}0$ and $R_\infty = 10^6$ the effect of transition movement is very small.

6.2. *Boundary-Layer Pressure Drag.*

The boundary-layer pressure drag $\Delta C_{Dp} = \Delta C_{Dp1} + \Delta C_{DpT}$ is presented in Figs. 17, 18 and 19 for $M_\infty = 1{\cdot}5$, $2{\cdot}5$ and $5{\cdot}0$. It will be noted that these results are plotted to a different scale from those for the overall skin-friction coefficient. The general shape of the curves, with minimum values for transition at about mid-chord, is much the same as described in Refs. 6 and 8 for the case of zero heat transfer. However, it is noticeable that the boundary-layer pressure drag decreases for the extreme transition positions with wall cooling and shows a smaller variation with transition position. This is because of the reduction of displacement thickness of the boundary layer with cooling. Further, when the cooling rate is high and the Mach number low, the value of δ_{tT}^* for the turbulent boundary layer may be greater than δ_{tT}^* for the laminar boundary layer and hence the normal sign of ΔC_{DpT} is reversed. The unusual behaviour when the Mach number is high and the Reynolds number low (*see* Fig. 19) is also of some interest. At a Mach number of 5 and Reynolds

number of 10^6 the rate of turbulent displacement-thickness growth is actually less than that of the laminar boundary layer over the forward part of the wing section except when the wall is highly cooled*. As a consequence the displacement effect of the boundary layer, and hence its pressure drag, increases as the transition point moves back in all cases except that of the highest cooling rate considered viz. $S_w = -0{\cdot}8$.

6.3. *Complete Boundary-Layer Drag C_{DB}.*

The complete boundary-layer drag results $C_{DB} = C_{F\infty} + \Delta C_{Dp}$ are presented in Figs. 20, 21 and 22. These overall results exhibit to an even more marked degree than did the skin-friction-coefficient results, a reduction in sensitivity to rearward movement of the transition point as the Mach number is increased and the Reynolds number is reduced. In the cases of zero heat transfer ($S_w = 0$) and the heated wall ($S_w = 0{\cdot}4$) at $M_\infty = 5{\cdot}0$, $R_\infty = 10^6$, Fig. 22, the drag is actually increased as the amount of laminar flow is increased. This is due to the combined effects of Mach number and Reynolds number on the skin friction and boundary-layer pressure drag previously discussed. It is evident, however, that for cooling to approximately free-stream temperature ($S_w \approx -0{\cdot}8$), there is still an appreciable reduction in drag with rearward movement of transition.

We can therefore infer that, in general, cooling the surface of a wing in flight increases its drag unless the boundary layers can be kept in a laminar state over much of their length. It will probably be necessary to cool the surfaces of an aircraft for flight at Mach numbers above about 3. With increase of skin friction there is an increase of heat transfer and so the amount of cooling needed is increased if the surface temperature is to be kept below a specified value. It may be noted that the power expended and extra weight required to provide the necessary cooling rapidly become factors of considerable importance with increase of Mach number in the performance of an aircraft. These considerations point to the need for preserving laminar flow at supersonic speeds and they underline the importance of research on methods to achieve this.

6.4. *The Effect of Wing Thickness.*

In Fig. 23 are plotted the ratios r_F and r_{DB} at a Reynolds number of 10^7 as functions of Mach number for the various values of the heat-transfer parameter S_w considered for the two cases of fully laminar and fully turbulent boundary layers. The ratio r_F is the ratio ($C_{F\infty}$ of 5% bi-convex wing)/($C_{F\infty}$ of flat plate) and r_{DB} is (C_{DB} of 5% bi-convex wing)/($C_{F\infty}$ of flat plate). It can reasonably be inferred from Fig. 9 of Ref. 6 that in general such ratios vary linearly with thickness-chord ratio for small changes of this latter ratio. It will be seen from Fig. 23 that both r_F and r_{DB} can differ from unity by quite large amounts with the boundary layer laminar, with the boundary layer turbulent they differ from unity by much smaller amounts of the same order as or less than those of incompressible flow. A marked reduction of these ratios occurs in all cases with a decrease of S_w, i.e. with an increase of wall cooling. Increase of Mach number, at least above about 3, results in an increase of these ratios.

The value of r_F and r_{DB} do not vary with Reynolds number with the boundary layer fully laminar but with the boundary layer turbulent it is found that both ratios decrease with increase of Reynolds number. The differences between these ratios and unity then decrease about 30 per cent as the Reynolds number increases from 10^6 to 10^7 but the decrease is much smaller (less than 10 per cent) as the Reynolds number increases from 10^7 to 10^8.

* It should of course be noted that at such a low value of R_∞ the chances of transition occurring well forward are remote in practice unless great efforts are made to stimulate turbulence artificially.

7. *Second-Order Effects on Skin Friction.*

In Ref. 6 an analysis as well as the results of a wide range of calculations are given for the secondary effect on the skin friction due to the reaction back on the boundary layer of the pressure and velocity changes produced by the boundary layer in the external flow for the case of zero heat transfer at the surface. The boundary layer causes an increase of pressure above that of purely inviscid flow proportional to $d\delta^*/dx$ to the first order, and this pressure increase therefore decreases from the front of the wing to the rear. Consequently, there is a local increase of $\rho_1 u_1^2$ (for M_1 greater than about 1·5) and a more negative pressure gradient than is predicted for purely inviscid flow. Both these effects combine to cause an increase of skin friction but with the boundary layer turbulent the pressure-gradient effect is much the smaller of the two. The resultant increase of skin friction varies roughly as the square of the Mach number and of course decreases with increase of Reynolds number. The calculations of Ref. 6 for the case of zero heat transfer showed that in the extreme case considered of $M_\infty = 5{\cdot}0$, $R_\infty = 10^6$ the skin friction of a 5% bi-convex wing was increased above that corresponding to the inviscid-flow pressure distribution by about 11% with the boundary layer fully turbulent and by about 5% with the boundary layer fully laminar.

Because of the considerable computational work involved a similar set of iterative calculations to determine these second-order effects was not undertaken for the present programme of cases involving heat transfer. However, an approximate analysis of which the details are given in Appendix I leads to the conclusion that at given values of R_∞ and M_∞ these effects are proportional to $(H\delta^*)$ at the trailing edge in the case of a fully laminar boundary layer and to δ^* at the trailing edge with the boundary layer turbulent. Thus, let us write

$$K_{2L} = (H\delta^*)_{S_w}/(H\delta^*)_0, \qquad \text{and} \qquad K_{2T} = (\delta^*)_{S_w}/(\delta^*)_0$$

where $(H\delta^*)_{S_w}$ is the value of $H\delta^*$ at the trailing edge obtained for a heat-transfer parameter S_w whilst $(H\delta^*)_0$ is the corresponding value when the heat transfer is zero, similarly $(\delta^*)_{S_w}$ and $(\delta^*)_0$ are the values of δ^* at the trailing edge for a heat-transfer parameter S_w and for $S_w = 0$, respectively. Then we infer from the above conclusion that we can write

$$\left.\begin{aligned} &\frac{(\Delta C_F^*)_{S_w}}{(\Delta C_F^*)_0} = K_{2L}, \text{ for a fully laminar boundary layer} \\ \text{and} \qquad &\frac{(\Delta C_F^*)_{S_w}}{(\Delta C_F^*)_0} = K_{2T}, \text{ for a fully turbulent boundary layer,} \end{aligned}\right\} \tag{25}$$

where ΔC_F^* denotes the fractional change in the skin-friction coefficient due to the change in pressure distribution produced by the boundary layer and the suffices S_w and 0 imply with heat transfer and without heat transfer, respectively.

However, at this stage a further point needs to be considered. It has already been noted in Section 1 that differences exist between the method used for the turbulent boundary layer in Ref. 6 and that of Spence[2] which has been used for the present calculations. These differences result in significant differences in the numerical results obtained only in the extreme cases considered of low Reynolds number and high Mach number, but for such cases these differences will also be reflected in significant differences of the second-order effects on skin friction. Before the results of Ref. 6 can be extended to cases of non-zero heat transfer by means of equations (25) above

it is necessary to modify those results to be appropriate to Spence's method. To do this we can again appeal to the conclusion arrived at in Appendix I and assume that

$$(\Delta C_F{}^*)_0 = (\Delta C_F{}^*)_{0,\text{ Ref. 6}} \frac{(\delta^*)_0}{(\delta^*)_{0,\text{ Ref. 6}}} \tag{26}$$

where $(\Delta C_F{}^*)_{0,\text{ Ref. 6}}$ is the value of the correction to the skin-friction coefficient for zero heat transfer given in Ref. 6, $(\delta^*)_{0,\text{ Ref. 6}}$ is the corresponding value of δ^* at the trailing edge and $(\delta^*)_0$ is the value of δ^* at the trailing edge as determined in the present calculations for zero heat transfer.

If K_1 denotes $(\delta^*)_0/(\delta^*)_{0,\text{ Ref. 6}}$ for the boundary layer fully turbulent then we have

$$\left.\begin{aligned} &\frac{(\Delta C_F{}^*)_0}{(\Delta C_F{}^*)_{0,\text{ Ref. 6}}} = K_1 \text{ when the boundary layer is fully turbulent} \\ &\text{and} \\ &(\Delta C_F{}^*)_0/(\Delta C_F{}^*)_{0,\text{ Ref. 6}} = 1 \text{ when the boundary layer is fully laminar.} \end{aligned}\right\} \tag{27}$$

Combining equations (25) and (27) we obtain

$$\left.\begin{aligned} &\left(\frac{\Delta C_F}{C_{F1\infty}}\right)_{S_w} = K_1 K_{2T} \left(\frac{\Delta C_F}{C_{F1\infty}}\right)_{0,\text{ Ref. 6}} \text{ with the boundary layer fully turbulent} \\ &\text{and} \\ &\left(\frac{\Delta C_F}{C_{F1\infty}}\right)_{S_w} = K_{2L} \left(\frac{\Delta C_F}{C_{F1\infty}}\right)_{0,\text{ Ref. 6}} \text{ with the boundary layer laminar} \end{aligned}\right\} \tag{28}$$

where $C_{F1\infty}$ is the initial skin-friction coefficient calculated for the inviscid-flow pressure distribution and $(\Delta C_F/C_{F1\infty})_{0,\text{ Ref. 6}}$ refers to the correction for the case of zero heat transfer as given in Fig. 1 of Ref. 6.

The value of K_1, K_{2L} and K_{2T} determined from these calculations for the flat plate are shown in Fig. 24 where K_1 is plotted as a function of R_∞ for various values of M_∞, and K_{2L} and K_{2T} are plotted as functions of S_w for various values of M_∞. The corresponding values for the bi-convex wing with $t/c = 0{\cdot}05$ were generally very close to those for the flat plate (particularly so for K_1 and K_{2T}) and there can be little loss of accuracy, bearing in mind the other approximations involved in the analysis, in accepting Fig. 24 as applicable over the range of t/c from 0 to 0·05.

To illustrate the order of the effect of heat transfer on the skin-friction increment the following table lists the value of $(\Delta C_F/C_{F1\infty}) \times 100$ for $M_\infty = 5{\cdot}0$ for the flat plate and the bi-convex aerofoil with the boundary layer fully turbulent and fully laminar:

$$\underline{(\Delta C_F/C_{F1\infty}) \times 100 \text{ for } M_\infty = 5{\cdot}0}$$

Flat plate $(t/c = 0)$

	$R_\infty = 10^6$		10^7		10^8	
S_w	Turb.	Lam.	Turb.	Lam.	Turb.	Lam.
−0·8	3·7	1·1	3·3	0·4	1·8	0·1
−0·4	4·3	2·9	3·8	0·9	2·7	0·3
0	4·8	5·5	4·2	1·7	3·0	0·6
+0·4	5·0	9·1	4·5	2·9	3·2	0·9

Bi-convex aerofoil ($t/c = 0{\cdot}05$)

	$R_\infty = 10^6$		10^7		10^8	
S_w	Turb.	Lam.	Turb.	Lam.	Turb.	Lam.
$-0{\cdot}8$	6·2	0·9	5·5	0·3	3·0	0·1
$-0{\cdot}4$	7·1	2·4	6·3	0·8	4·5	0·2
0	7·9	4·6	7·0	1·5	5·1	0·5
$+4{\cdot}4$	8·4	7·6	7·5	2·4	5·3	0·8

However, a point which can readily be overlooked must here be stressed. In the case of the laminar boundary layer the theory is essentially complete and free of empirical elements. The above correction can therefore be applied without further reservation, thus the final skin-friction coefficient is

$$C_{F\infty} = C_{F1\infty} + \Delta C_F.$$

On the other hand, in the case of the turbulent boundary layer an essential element of the theory used is the mean enthalpy concept for which the constants have been adjusted to give as good agreement as possible with available data derived from measurements on flat plates and on cylinders with their generators aligned with the stream, i.e. zero pressure-gradient conditions if the flow were inviscid. Most of these measurements have been made with the heat transfer small or zero, for Reynolds numbers in the region of 10^7 and Mach numbers less than about 4, although there are a few measurements made under other conditions of Mach number, Reynolds number and heat transfer. These measurements generally lend good support to the mean enthalpy concept, but as already noted in Section 1 many more reliable measurements are required before the range of validity of this concept can be completely assessed. If for the present we accept the concept with the constants proposed by Sommer and Short as leading to correct values of the skin friction for a flat plate at zero incidence with a fully turbulent boundary layer for the ranges of Mach number, Reynolds number and heat-transfer parameter, S_w, considered here, then it can be inferred that the second-order interaction effect is implicitly included when the inviscid-flow pressure gradient is zero. It follows that for the aerofoil with the boundary layer turbulent the full correction described above should not be applied but only the difference between the correction for the aerofoil and that for the flat plate.

It is suggested that the ratio $(\Delta C_F/C_{F\infty})$ can be assumed to vary linearly with x_T/c, the transition position, between the value for $x_T/c = 0$ (fully turbulent boundary layer) and the value $x_T/c = 1{\cdot}0$ (fully laminar boundary layer) for the purpose of estimating the correction for intermediate positions of the transition.

8. *The Effects of Small Changes of ω and σ.*

Fig. 25 shows the chordwise distributions of the skin-friction coefficient with the boundary layer laminar for the bi-convex wing at a Mach number of 5 for $S_w = 0$ (zero heat transfer) and $S_w = 0{\cdot}4$ and for values of ω of $0{\cdot}89$ and $0{\cdot}65$, with the value of σ kept at $0{\cdot}725$. As explained in Section 1 the smaller value of ω is about the lowest value that need be considered for the purposes of this investigation. It will be seen that the skin-friction coefficient is decreased with a change of ω from $0{\cdot}89$ to $0{\cdot}65$ by about 13 to 17% for $S_w = 0$ and by about 16 to 20% for $S_w = 0{\cdot}4$.

In Ref. 12 a detailed analysis is offered of the effects of small changes of ω and σ on skin friction. It is there shown that the formula {equation (21)} quoted in Section 4 for the skin friction in the laminar boundary layer on a flat plate at zero incidence leads to very nearly the same reductions in skin-friction coefficient as are shown in Fig. 25 associated with the same reduction of ω at the same values of S_w. It is also shown in Ref. 12 that the effects of changes of σ in the absence of a pressure gradient and with wall temperature unchanged are very small and for any likely change of σ for air over the ranges of the parameters considered here these effects will be generally negligible. Further analysis of the results presented in Ref. 1 for the combined effects of changes of ω and σ with both positive and negative pressure gradients and the boundary layer laminar leads to the general conclusion that in all cases and with given wall temperatures the percentage changes of skin friction due to small changes of ω and σ can be predicted with adequate accuracy from the flat-plate formula {equation (21)}. As noted above the effects of small changes of σ are then very small, but it must be pointed out that *for constant* S_w a small change in σ can result in a significant change in wall temperature and hence in a marked change of skin friction particularly in the presence of a pressure gradient (*see* Figs. 9 and 12 of Ref. 1).

Since the turbulent boundary layer can be expected to be less sensitive to pressure-gradient effects than the laminar boundary layer it seems reasonable to conclude that the percentage changes of skin friction due to small changes of ω and σ will also be predicted with adequate accuracy by the corresponding flat-plate formula of Section 4 {equation (24)}. The details of the resulting analysis for the turbulent boundary layer are also given in Ref. 12 where it is shown that the effects of changes of ω are generally about a third of those for the laminar boundary layer and that again the effects of likely changes of σ for air with the wall temperature unchanged are small.

9. *Conclusions.*

Results have been presented for the calculated boundary-layer drag and its constituents for a flat plate and a 5% thick bi-convex wing at zero incidence for wide ranges of Mach number, Reynolds number, transition position and heat-transfer conditions.

These results have been analysed to establish in physical terms the separate and combined effects of heat transfer and pressure gradient on the boundary-layer characteristics. It is shown that in the absence of any pressure gradient the skin friction with the boundary layer laminar is much less sensitive to changes of wall temperature and Mach number than is the skin friction with the boundary layer turbulent. In the former case the effects of the changes of density, viscosity and velocity distribution near the wall associated with wall temperature changes almost nullify each other; in the latter case the density changes are dominant so that the skin friction decreases readily with increase of wall temperature. On the other hand, the laminar boundary layer is much more sensitive to the effects of pressure gradient; with a favourable pressure gradient the skin friction increases readily with increase of wall temperature and *vice versa*. This can be explained in terms of the heightened response of the air near the wall to the pressure gradients when its density is reduced by wall heating and *vice versa*. This effect is much less apparent with the boundary layer turbulent due to the relative insensitivity of its velocity profile to pressure gradients.

It is shown that the effects of rearward movement of transition on skin friction and boundary-layer drag are reduced by increase of Mach number, reduction of Reynolds number and increase of wall temperature. In the extreme case considered of $M_\infty = 5{\cdot}0$, $R_\infty = 10^6$ and $S_w = 0{\cdot}4$ the

boundary-layer drag of the aerofoil actually increases as the transition position moves aft, but this case can hardly be regarded as likely to arise in practice full scale.

In general cooling of the surface causes an increase of drag for all transition positions except for those very close to the trailing edge. We may expect that such cooling will probably be necessary for aircraft designed to fly at Mach numbers above about 3·0. The degree of cooling required will increase with the heat-transfer rate and this in turn can be expected to be directly related to the skin-friction drag*. It can be inferred, therefore, that both on the grounds of drag as well as the weight and complexity incurred by the cooling installation the penalty of having the boundary layer turbulent rather than laminar will rapidly increase with increase of Mach number. The importance of future research into means for preserving extensive regions of laminar flow at high Mach numbers cannot therefore be too strongly stressed.

The paper includes brief discussions of the effects of the interaction between the boundary layer and the external flow on the skin-friction drag and of the effects of small changes of Prandtl number and the viscosity-temperature index.

* A forthcoming paper by R. E. Luxton will deal with this point in more detail.

NOTATION

a	Velocity of sound
c	Chord
c_p	Specific heat at constant pressure
c_f	Local skin-friction coefficient based on leading-edge conditions $= 2\tau_w/\rho_a u_a^2$
$(c_f)_{\text{local}}$	Skin-friction coefficient based on local conditions $= 2\tau_w/\rho_1 u_1^2$
f	Value of δ_1/θ
f_z	Value of δ_1/θ in a zero pressure gradient
g_n	Function defined in equation (8)
k	Coefficient of thermal conductivity
k_1	Correction factor in equation (5)
k_2	Correction factor in equation (2)
p	Pressure
r_F	($C_{F\infty}$ for wing)/($C_{F\infty}$ for flat plate)
r_{DB}	(C_{DB} for wing)/($C_{F\infty}$ for flat plate)
t	Thickness
u	Velocity in x direction
x	Distance measured along the surface
y	Distance measured normal to the surface
B	Index in equation (15); also $(M_\infty^2-1)^{1/2}$
C_{Fa}	Overall skin-friction coefficient based on leading-edge conditions
$C_{F\infty}$	Overall skin-friction coefficient based on undisturbed stream conditions
ΔC_F	Change in $C_{F\infty}$ due to interaction of boundary layer and external flow
ΔC_F^*	$= \Delta C_F/C_{F1\infty}$
C_{DB}	Boundary-layer drag coefficient $= C_{F\infty} + \Delta C_{Dp}$
C_p	Pressure coefficient
F	Function of Mach number, equation (15)
G	Function of Mach number, equation (15)
H	Form factor $= \delta^*/\theta$
K_T	Constant in equation (15)
M	Mach number
R	Reynolds number; suffices indicate values on which R is based
S	Temperature-ratio parameter $= T/T_r - 1$
T	Absolute temperature
T_r	Recovery temperature, i.e. wall temperature for zero heat transfer
T_m	'Intermediate' temperature, *see* equations (13) and (23)

NOTATION—*continued*

Y	Transformed y co-ordinate, equation (1)
β	Surface slope
γ	Ratio of specific heats
δ	Value of y defining outer edge of boundary layer
δ_1	Value of Y corresponding to $y = \delta$
δ^*	Displacement thickness
η	Transformed y co-ordinate, equation (11)
θ	Momentum thickness
μ	Coefficient of viscosity
ν	Kinematic viscosity
ρ	Density
σ	Prandtl number $= \mu C_p/k$
τ	Shear stress
ω	Temperature-viscosity relationship index
Δ	Value of η corresponding to $y = \delta$
ΔC_{Dp}	Boundary-layer pressure drag $= \Delta C_{Dp1} + \Delta C_{DpT}$
ΔC_{Dp1}	Contribution of displacement thickness to ΔC_{Dp}
ΔC_{DpT}	Contribution of transition point to ΔC_{Dp}
Λ	Pressure-gradient parameter, equation (3)

Suffices

a	Reference conditions in the free stream at L.E. just after shock (if any)
∞	Reference conditions in the undisturbed stream
i	Incompressible flow
o	Stagnation conditions; also zero-heat-transfer conditions
S_w	Conditions corresponding to heat-transfer parameter S_w
1	Values at outer edge of boundary layer; also sometimes used to distinguish values of skin friction calculated without allowance for second-order interaction effects of boundary layer and external flow
T	Transition point
w	Wall values
l	Laminar flow
t	Turbulent flow
n, $n + 1$, etc.	Values at x_n, x_{n+1} etc.
z	Conditions of zero pressure gradient

REFERENCES

No.	Author(s)	Title, etc.
1	R. E. Luxton and A. D. Young ..	Generalised methods for the calculation of laminar compressible boundary-layer characteristics with heat transfer and non-uniform pressure distribution. A.R.C. R. & M. 3233. January, 1960.
2	D. A. Spence	The growth of compressible turbulent boundary layers on isothermal and adiabatic walls. A.R.C. R. & M. 3191. June, 1959.
3	S. C. Sommer and Barbara J. Short	Free-flight measurements of skin friction of turbulent boundary layers with high rates of heat transfer at high supersonic speeds. *J. Ae. Sci.*, Vol. 23, No. 6, p. 536. June, 1956.
4	F. W. Matting, D. R. Chapman, J. R. Nyholm and A. G. Thomas	Turbulent skin friction at high Mach numbers and Reynolds numbers. Heat Transfer and Fluid Mechanics Inst. Symposium, Los Angeles. June, 1959.
5	A. D. Young	The calculation of the profile drag of aerofoils and bodies of revolution at supersonic speeds. Coll. of Aeronautics, Cranfield, Report 73. April, 1953.
6	A. D. Young and S. Kirkby ..	Effects of interaction between boundary layers and external stream and of incidence on boundary-layer drag at supersonic speeds. A.R.C. C.P. 451. November, 1958.
7	A. D. Young and S. Kirkby ..	The profile drag of bi-convex and double wedge wing sections at supersonic speeds. Symposium on Boundary Layer Effects in Aerodynamics, N.P.L. 1955. (H.M.S.O.).
8	A. D. Young and S. Kirkby ..	The profile drag of bi-convex wing sections at supersonic speeds. *50 Jahre Grengschichtforschung*. H. Gortler and W. Tollmien (editors). Verlag. Friedr. Vieweg and Sohn, Braunschweig. 1955.
9	A. D. Young	Skin friction in the laminar boundary layer in compressible flow. Coll. of Aeronautics Report 20. 1948. Also *Aero. Quart.*, Vol. 1, Part 2, pp. 137 to 164. August, 1949.
10	W. J. Duncan, A. S. Thom and A. D. Young	*Mechanics of fluids*. Arnold Ltd. (editors). 1960.
11	G. E. Gadd, D. W. Holder and J. D. Regan	An experimental investigation of the interaction between shock waves and boundary layers. *Proc. Roy. Soc.* A, Vol. 226, p. 227. 1954.
12	A. D. Young	The effects of small changes of the Prandtl number and the viscosity-temperature index on skin friction. *Aero. Quart.*, Vol. XV, pp. 392 to 406. November, 1964.
13	B. S. Stratford and G. S. Beavers	The calculation of the compressible turbulent boundary layer in an arbitrary pressure gradient—a correlation of certain previous methods. A.R.C. R. & M. 3207. September, 1959.
14	J. O. Hirschfelder, C. F. Curtiss and R. B. Bird	*Molecular theory of gases and liquids*. John Wiley & Sons, Inc., New York. 1954.

APPENDIX

Approximate Analysis of the Second-Order Effect on Skin-Friction Drag with Heat Transfer

In this appendix we will consider first a flat plate at zero incidence and we will denote quantities obtained in the first-stage calculation, i.e. with zero pressure gradient, by suffix z, and increments of quantities between the first and second stages will be denoted by the prefix Δ. For consistency with the main text we will continue to denote the *overall* skin-friction coefficient based on undisturbed stream conditions for the first stage by $C_{F1\infty}$.

With the boundary layer laminar the approximate analysis given in Appendix I of Ref. 6 for the case of zero heat transfer applies essentially unchanged to the case with heat transfer. In the notation here adopted equation A.24 of that reference can be written

$$\Delta C_F{}^* = \frac{\Delta C_F}{C_{F1\infty}} = \frac{\text{const. } H_z^2}{B_z(R_\infty f_z)^{1/2}}$$

$$= \text{const. } (H_z \delta_z{}^*)_{\text{T.E.}}, \tag{A.1}$$

for a given main-stream Mach number, where suffix T.E. denotes that the quantities are evaluated at the trailing edge. It follows that we can write the ratio of $\Delta C_F{}^*$ with heat-transfer parameter S_w to $\Delta C_F{}^*$ with zero heat transfer

$$\frac{(\Delta C_F{}^*)_{S_w}}{(\Delta C_F{}^*)_0} = \frac{[(H_z \delta_z{}^*)_{\text{T.E.}}]_{S_w}}{[(H_z \delta_z{}^*)_{\text{T.E.}}]_0}. \tag{A.2}$$

It seems plausible, as we are dealing here with small corrections, to assume that we can generalise this result to thin wing sections by writing

$$\frac{(\Delta C_F{}^*)_{Sw}}{(\Delta C_F{}^*)_0} = \frac{[(H\delta^*)_{\text{T.E.}}]_{S_w}}{[(H\delta^*)_{\text{T.E.}}]_0} \tag{A.3}$$

where it is understood that the values of H and δ^* on the right-hand side are those evaluated in the first stage without taking interaction effects into account.

It may be noted that examination of the momentum integral equation as in the analysis that follows for the turbulent boundary shows that the factors that contribute to the local skin-friction coefficient increment fall into two groups, namely, those due to the induced pressure gradients and the associated velocity and density gradients and those due to the changes in the dynamic pressure $\rho_1 u_1{}^2$. With the boundary layer laminar the contribution of the former can be shown to be proportional to $(H_z + 2 - M_\infty{}^2) d\delta^*/dx$ and that of the latter is proportional to $-(2 - M_\infty{}^2) d\delta^*/dx$. The result on which equation (A.1) above is based then follows.

With the boundary layer fully turbulent on a flat plate at zero incidence we can write {*see* equation (24)}

$$\frac{\theta_z}{x} = 0{\cdot}0225 \frac{T_{mt}{}^{-(5-\omega)/6}}{T_\infty} R_x{}^{-1/6} \tag{A.4}$$

where $R_x = u_\infty x/\nu_\infty$. Also (*see* Ref. 6) the pressure, velocity and density increments associated with the interaction of boundary layer and external flow are given by

$$\left.\begin{aligned} \Delta p/\rho_\infty u_\infty^2 &= \frac{H_z}{B_z}\frac{d\theta_z}{dx} \\ \text{where} \qquad B_z &= (M_\infty^2-1)^{1/2}, \\ \Delta u_1/u_\infty &= (u_1-u_\infty)/u_\infty = -\frac{H_z}{B_z}\frac{d\theta_z}{dx} \\ \text{and} \qquad \Delta\rho_1/\rho_\infty &= (\rho_1-\rho_\infty)/\rho_\infty = -M_\infty^2\Delta u_1/u_\infty . \end{aligned}\right\} \tag{A.5}$$

The momentum integral equation of the boundary layer is

$$\frac{\tau_w}{\rho_1 u_1^2} = \theta' + \theta\left[(H+2)\frac{u_1'}{u_1} + \frac{\rho_1'}{\rho_1}\right] \tag{A.6}$$

where the accent denotes differentiation with respect to x. Hence to the first order the change in τ_w due to the interaction effect can be written

$$\Delta\tau_w = \rho_\infty u_\infty^2\left[\frac{d}{dx}(\Delta\theta) + \frac{\theta}{u_\infty}(H_z+2)\frac{d}{dx}(\Delta u_1) + \frac{\theta}{\rho_\infty}\frac{d}{dx}(\Delta\rho_1)\right] + \theta'_z\rho_\infty u_\infty^2\left[\frac{\Delta\rho_1}{\rho_\infty} + \frac{2\Delta u_1}{u_\infty}\right].$$

It follows that

$$\frac{\Delta C_{f\infty}}{C_{f\infty}} = \frac{1}{\theta_z'}\frac{d}{dx}(\Delta\theta) + \frac{\theta_z}{\theta_z'}\left[(H_z+2)\frac{d}{dx}\left(\frac{\Delta u_1}{u_\infty}\right) + \frac{d}{dx}\left(\frac{\Delta\rho_1}{\rho_\infty}\right)\right] + \frac{\Delta\rho_1}{\rho_\infty} + 2\frac{\Delta u_1}{u_\infty}.$$

Here the last two terms arise from the change in $\rho_1 u_1^2$ due to interaction effects, the remaining terms derive from the induced gradients in θ and pressure. With the aid of equations (A.5) this equation can be written

$$\frac{\Delta C_{f\infty}}{C_{f\infty}} = \frac{1}{\theta_z'}\frac{d}{dx}(\Delta\theta) - \frac{\theta_z}{\theta_z'}\left[(H_z+2-M_\infty^2)\frac{H_z}{\theta_z}\theta_z''\right] - (2-M_\infty^2)\frac{H_z}{B_z}\theta_z'$$

and this becomes with the aid of equation (A.4)

$$\frac{\Delta C_{f\infty}}{C_{f\infty}} = \frac{1}{\theta_z'}\frac{d}{dx}(\Delta\theta) + \frac{H_z\theta_z}{6B_z x}[H_z - 8 + 4M_\infty^2]. \tag{A.7}$$

The factor $(H_z-8+4M_\infty^2)$ on the right-hand side of this equation is about 100 at $M_\infty = 5$ and about 21 at $M_\infty = 2{\cdot}5$ and being largely dominated by the term $4M_\infty^2$ it varies relatively little with S_w. The first term on the right-hand side can be similarly expressed as

$$\frac{1}{\theta_z'}\frac{d}{dx}(\Delta\theta) = \frac{2}{15}\frac{H_z}{B_z}\frac{\theta_z}{x}[M_\infty^2\omega(\gamma-1) - H_z - 1]$$

when use is made of the expression for $\Delta\theta$ given in equation A.28 of Ref. 6. With $\omega = 0{\cdot}89$, and $\gamma = 1{\cdot}4$ this term is found to be small compared with the second term on the right-hand side of equation (A.7). This is linked with the fact that for the turbulent boundary layer the dominant effect of the interaction between the boundary layer and main-stream flow derives from the accompanying effect on the dynamic pressure, $\rho_1 u_1^2$, the effects of the changes in the pressure and momentum gradients being relatively small.

However, we can now write equation (A.7) in the form

$$\frac{\Delta C_{f\infty}}{C_{f\infty}} = \frac{H_z\theta_z}{30B_z x}[21{\cdot}42\,M_\infty{}^2 + H_z - 44] \tag{A.8}$$

with $\omega = 0{\cdot}89$, and sample calculations show immediately that the term in square brackets varies by less than 1% over the range of S_w considered for $M_\infty = 5{\cdot}0$ and for $M_\infty = 2{\cdot}5$ the variation is no more than 4%.

It follows that we can write with good approximation,

$$\frac{\Delta C_{f\infty}}{C_{f\infty}} = C_1(M_\infty)H_z\theta_z'$$

where C_1 is a constant for a given main-stream Mach number and is independent of S_w. This then leads to the result

$$\Delta C_F{}^* = \frac{\Delta C_F}{C_{F1\infty}} = C_2(M_\infty)\delta_z{}^*{}_{\text{T.E.}} \tag{A.9}$$

where C_2 is another function of M_∞, only.

It follows that with the boundary layer turbulent

$$\frac{(\Delta C_F{}^*)_{S_w}}{(\Delta C_F{}^*)_0} = \frac{(\delta_z{}^*{}_{\text{T.E.}})_{S_w}}{(\delta_z{}^*{}_{\text{T.E.}})_0} \tag{A.10}$$

and it is again assumed that this can be generalised for thin wing sections in the form

$$\frac{(\Delta C_F{}^*)_{S_w}}{(\Delta C_F{}^*)_0} = \frac{(\delta^*{}_{\text{T.E.}})_{S_w}}{(\delta^*{}_{\text{T.E.}})_0} \tag{A.11}$$

where it is understood as before that the values of δ^* on the right-hand side are as evaluated without taking interaction effects into account.

TABLE 1

Skin-Friction Drag of Flat Plate at Zero Incidence (One Surface). No Interaction Effects

M_∞	S_w	R_∞	Laminar B.L. $C_{F\infty} \times 10^3$	Turbulent B.L. $C_{F\infty} \times 10^3$
1·0	+0·4	10^6	1·305	3·705
		10^7	0·412	2·523
		10^8	0·131	1·723
	0	10^6	1·320	4·174
		10^7	0·416	2·841
		10^8	0·132	1·939
	−0·4	10^6	1·338	4·824
		10^7	0·422	3·253
		10^8	0·134	2·220
	−0·8	10^6	1·365	5·791
		10^7	0·432	3·944
		10^8	0·137	2·693
2·5	+0·4	10^6	1·271	2·650
		10^7	0·401	1·803
		10^8	0·127	1·231
	0	10^6	1·287	3·046
		10^7	0·406	2·074
		10^8	0·129	1·416
	−0·4	10^6	1·308	3·630
		10^7	0·413	2·471
		10^8	0·131	1·686
	−0·8	10^6	1·338	4·598
		10^7	0·422	3·133
		10^8	0·134	2·141
5·0	+0·4	10^6	1·212	1·518
		10^7	0·383	1·033
		10^8	0·121	0·708
	0	10^6	1·229	1·773
		10^7	0·388	1·217
		10^8	0·123	0·831
	−0·4	10^6	1·251	2·166
		10^7	0·395	1·474
		10^8	0·125	1·006
	−0·8	10^6	1·286	2·879
		10^7	0·406	1·959
		10^8	0·129	1·338

Note to Table 1

These results are based on the following formulae.

Laminar Flow

$$C_{F\infty}\sqrt{R_\infty} = 1{\cdot}328\left(\frac{T_{ml}}{T_\infty}\right)^{-(1-\omega)/2}$$

where

$$T_{ml} = T_\infty\left[0{\cdot}45 + 0{\cdot}55\,\frac{T_w}{T_\infty} + 0{\cdot}09\,(\gamma-1)M_\infty{}^2\sigma^{1/2}\right]$$

$$= 0{\cdot}45\,T_\infty + 0{\cdot}55\,T_w + 0{\cdot}18\,(T_r - T_\infty)$$

Turbulent Flow

$$C_{F\infty}R_\infty{}^{1/6} = 0{\cdot}04500\,(T_{ml}/T_\infty)^{-(5-\omega)/6}$$

where

$$T_{ml} = T_\infty\left[0{\cdot}55 + 0{\cdot}45\,\frac{T_w}{T_\infty} + 0{\cdot}035\,M_1{}^2\right]$$

$$= 0{\cdot}55\,T_\infty + 0{\cdot}45\,T_w + 0{\cdot}195\,(T_r - T_\infty)$$

with

$$\sigma = 0{\cdot}725 \text{ and taking } T_r = T_\infty\left[1 + \frac{(\gamma-1)}{2}\,M_1{}^2\sigma^{1/3}\right]$$

The value of ω in the above is taken as $0{\cdot}89$.

TABLE 2

Calculated Results for Bi-convex Wings ($t/c = 0{\cdot}05$) (One Surface). No Interaction Effects

M_∞	S_w	$\frac{x_T}{c}$	R_∞	$\Delta C_{Dpl} \times 10^3$	$\Delta C_{DpT} \times 10^3$	$C_{F\infty} \times 10^3$	$C_{DB} \times 10^3$
1·5	+0·4	0·05	10^6	+0·1924	−0·0579	3·478	3·612
			10^7	+0·0994	−0·0183	2·302	2·383
			10^8	+0·0586	−0·0058	1·553	1·606
		0·25	10^6	+0·1696	−0·0620	3·186	3·293
			10^7	+0·0174	−0·0196	1·967	1·965
			10^8	−0·0182	−0·0062	1·284	1·260
		0·75	10^6	+0·1353	+0·0806	2·297	2·513
			10^7	−0·0258	+0·0255	1·072	1·072
			10^8	−0·0565	+0·0081	0·585	0·537
		1·00	10^6	+0·2293	+0·1660	1·817	2·213
			10^7	+0·0725	+0·0525	0·575	0·700
			10^8	+0·0229	+0·0166	0·182	0·221
1·5	0	0·05	10^6	+0·1409	−0·0412	3·890	3·989
			10^7	+0·0728	−0·0130	2·587	2·647
			10^8	+0·0430	−0·0041	1·750	1·789
		0·25	10^6	+0·0980	−0·0411	3·500	3·557
			10^7	−0·0042	−0·0130	2·192	2·175
			10^8	−0·0246	−0·0041	1·442	1·413
		0·75	10^6	+0·0708	+0·0475	2·339	2·458
			10^7	−0·0374	+0·0150	1·134	1·111
			10^8	−0·0540	+0·0047	0·638	0·589
		1·00	10^6	+0·1664	+0·0929	1·713	1·972
			10^7	+0·0526	+0·0294	0·542	0·624
			10^8	+0·0166	+0·0093	0·171	0·197
1·5	−0·4	0·05	10^6	+0·0844	−0·0249	4·469	4·528
			10^7	+0·0429	−0·0079	2·986	3·021
			10^8	+0·0250	−0·0025	2·025	2·047
		0·25	10^6	+0·0322	−0·0225	3·951	3·960
			10^7	−0·0225	−0·0071	2·512	2·482
			10^8	−0·0289	−0·0023	1·664	1·633
		0·75	10^6	+0·0156	+0·0193	2·430	2·465
			10^7	−0·0434	+0·0061	1·231	1·193
			10^8	−0·0476	+0·0019	0·717	0·671
		1·00	10^6	+0·1075	+0·0304	1·602	1·740
			10^7	+0·0340	+0·0096	0·507	0·550
			10^8	+0·0108	+0·0030	0·160	0·174

TABLE 2—*continued*

M_∞	S_w	$\frac{x_T}{c}$	R_∞	$\Delta C_{Dp1} \times 10^3$	$\Delta C_{DpT} \times 10^3$	$C_{F\infty} \times 10^3$	$C_{DB} \times 10^3$
1·5	−0·8	0·05	10^6	+0·0255	−0·0085	5·371	5·388
			10^7	+0·0113	−0·0027	3·608	3·616
			10^8	+0·0060	−0·0009	2·452	2·457
		0·25	10^6	−0·0189	−0·0052	4·667	4·642
			10^7	−0·0310	−0·0016	3·014	2·981
			10^8	−0·0266	−0·0005	2·012	1·985
		0·75	10^6	−0·0235	−0·0040	2·621	2·593
			10^7	−0·0387	−0·0013	1·399	1·359
			10^8	−0·0342	−0·0004	0·846	0·811
		1·00	10^6	+0·0483	−0·0191	1·491	1·520
			10^7	+0·0153	−0·0061	0·471	0·481
			10^8	+0·0048	−0·0019	0·149	0·152
2·5	+0·4	0·05	10^6	+0·1121	−0·0395	2·809	2·881
			10^7	+0·0515	−0·0125	1·840	1·879
			10^8	+0·0279	−0·0040	1·237	1·260
		0·25	10^6	+0·1246	−0·0480	2·578	2·655
			10^7	+0·0058	−0·0152	1·545	1·536
			10^8	−0·0204	−0·0048	0·994	0·969
		0·75	10^6	+0·1210	+0·0678	1·922	2·111
			10^7	−0·0063	+0·0214	0·845	0·860
			10^8	−0·0339	+0·0068	0·438	0·411
		1·00	10^6	+0·1622	+0·1415	1·634	1·938
			10^7	+0·0513	+0·0448	0·517	0·613
			10^8	+0·0162	+0·0142	0·163	0·194
2·5	0	0·05	10^6	+0·0787	−0·0287	3·180	3·230
			10^7	+0·0351	−0·0091	2·096	2·122
			10^8	+0·0186	−0·0029	1·412	1·428
		0·25	10^6	+0·0696	−0·0330	2·859	2·895
			10^7	−0·0113	−0·0104	1·742	1·720
			10^8	−0·0257	−0·0033	1·131	1·102
		0·75	10^6	+0·0693	+0·0409	1·992	2·103
			10^7	−0·0187	+0·0129	0·903	0·935
			10^8	−0·0349	+0·0041	0·482	0·451
		1·00	10^6	+0·1234	+0·0793	1·605	1·807
			10^7	+0·0390	+0·0251	0·507	0·572
			10^8	+0·0123	+0·0079	0·161	0·181

TABLE 2—*continued*

M_∞	S_w	$\frac{x_T}{c}$	R_∞	$\Delta C_{Dp1} \times 10^3$	$\Delta C_{DpT} \times 10^3$	$C_{F\infty} \times 10^3$	$C_{DB} \times 10^3$
2·5	−0·4	0·05	10^6	+0·0455	−0·0178	3·715	3·743
			10^7	+0·0188	−0·0056	2·465	2·478
			10^8	+0·0093	−0·0018	1·667	1·674
		0·25	10^6	+0·0206	−0·0193	3·263	3·264
			10^7	−0·0248	−0·0061	2·027	1·996
			10^8	−0·0288	−0·0019	1·329	1·298
		0·75	10^6	+0·0242	+0·0186	2·074	2·117
			10^7	−0·0276	+0·0059	0·984	0·963
			10^8	−0·0338	+0·0019	0·546	0·515
		1·00	10^6	+0·0861	+0·0286	1·529	1·643
			10^7	+0·0272	+0·0090	0·483	0·520
			10^8	+0·0086	+0·0029	0·153	0·164
2·5	−0·8	0·05	10^6	+0·0118	−0·0069	4·603	4·608
			10^7	+0·0021	−0·0022	3·075	3·075
			10^8	−0·0002	−0·0007	2·087	2·086
		0·25	10^6	−0·0203	−0·0062	3·945	3·918
			10^7	−0·0331	−0·0020	2·502	2·467
			10^8	−0·0284	−0·0006	1·657	1·628
		0·75	10^6	−0·0130	+0·0002	2·253	2·240
			10^7	−0·0313	+0·0001	1·133	1·102
			10^8	−0·0292	+0·0000	0·658	0·629
		1·00	10^6	+0·0468	−0·0106	1·456	1·492
			10^7	+0·0148	−0·0033	0·461	0·472
			10^8	+0·0047	−0·0011	0·146	0·149
5·0	+0·4	0·05	10^6	+0·1324	−0·0496	1·747	1·830
			10^7	+0·0528	−0·0157	1·095	1·132
			10^8	+0·0251	−0·0050	0·721	0·741
		0·25	10^6	+0·2369	−0·0637	1·751	1·924
			10^7	+0·0428	−0·0201	0·932	0·955
			10^8	−0·0079	−0·0064	0·560	0·546
		0·75	10^6	+0·2450	+0·0835	1·694	2·023
			10^7	+0·0495	+0·0264	0·631	0·707
			10^8	−0·0052	+0·0084	0·270	0·273
		1·00	10^6	+0·2161	+0·1657	1·715	2·097
			10^7	+0·0683	+0·0524	0·542	0·663
			10^8	+0·0216	+0·0166	0·172	0·210

TABLE 2—*continued*

M_∞	S_w	$\frac{x_T}{c}$	R_∞	$\Delta C_{Dp1} \times 10^3$	$\Delta C_{DpT} \times 10^3$	$C_{F\infty} \times 10^3$	$C_{DB} \times 10^3$
5·0	0	0·05	10^6	+0·0931	−0·0364	1·986	2·043
			10^7	+0·0350	−0·0115	1·261	1·285
			10^8	+0·0156	−0·0036	0·836	0·848
		0·25	10^6	+0·1531	−0·0439	1·906	2·015
			10^7	+0·0148	−0·0139	1·046	1·047
			10^8	−0·0179	−0·0044	0·641	0·619
		0·75	10^6	+0·1656	+0·0456	1·675	1·887
			10^7	+0·0255	+0·0144	0·642	0·682
			10^8	−0·0118	+0·0046	0·286	0·279
		1·00	10^6	+0·1730	+0·0745	1·631	1·878
			10^7	+0·0547	+0·0235	0·516	0·594
			10^8	+0·0173	+0·0074	0·163	0·188
5·0	−0·4	0·05	10^6	+0·0537	−0·0232	2·353	2·383
			10^7	+0·0170	−0·0073	1·515	1·525
			10^8	+0·0060	−0·0023	1·011	1·015
		0·25	10^6	+0·0747	−0·0261	2·151	2·200
			10^7	−0·0108	−0·0082	1·223	1·204
			10^8	−0·0266	−0·0026	0·760	0·730
		0·75	10^6	+0·0938	+0·0158	1·679	1·789
			10^7	+0·0043	+0·0050	0·670	0·680
			10^8	−0·0173	+0·0016	0·315	0·299
		1·00	10^6	+0·1344	+0·0024	1·544	1·680
			10^7	+0·0425	+0·0007	0·488	0·531
			10^8	+0·0134	+0·0002	0·154	0·168
5·0	−0·8	0·05	10^6	+0·0145	−0·0098	3·028	3·032
			10^7	−0·0010	−0·0031	1·981	1·977
			10^8	−0·0037	−0·0010	1·333	1·328
		0·25	10^6	+0·0022	−0·0093	2·621	2·614
			10^7	−0·0333	−0·0029	1·555	1·519
			10^8	−0·0335	−0·0009	0·997	0·963
		0·75	10^6	+0·0278	−0·0059	1·746	1·768
			10^7	−0·0145	−0·0019	0·743	0·727
			10^8	−0·0216	−0·0006	0·375	0·353
		1·00	10^6	+0·0886	−0·0424	1·461	1·507
			10^7	+0·0280	−0·0134	0·462	0·477
			10^8	+0·0089	−0·0042	0·146	0·151

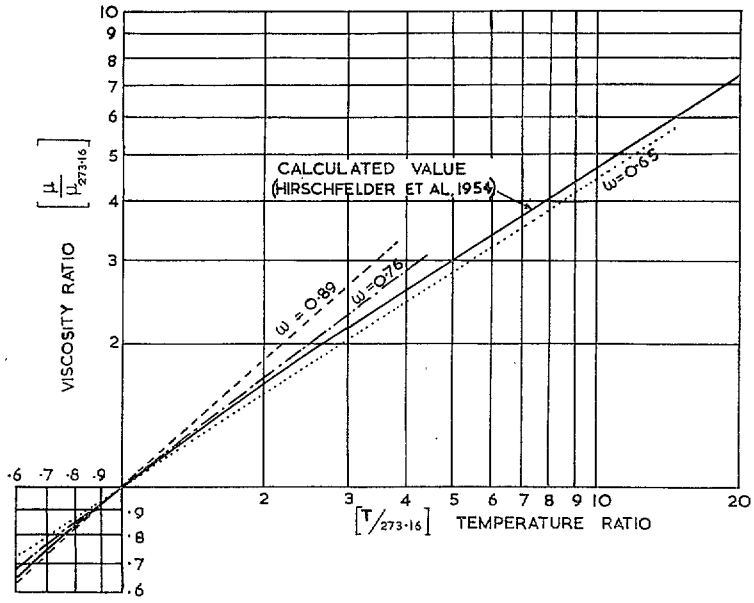

FIG. 1. Calculated variation of viscosity with temperature for air.

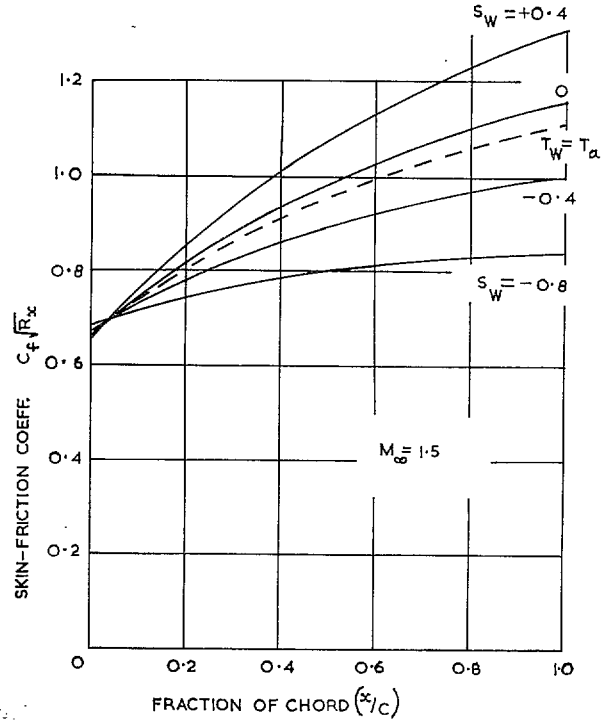

FIG. 2. Effect of wall temperature ratio, 5% thick bi-convex wing section: $M_\infty = 1\cdot5$, $x_T/c = 1\cdot0$.

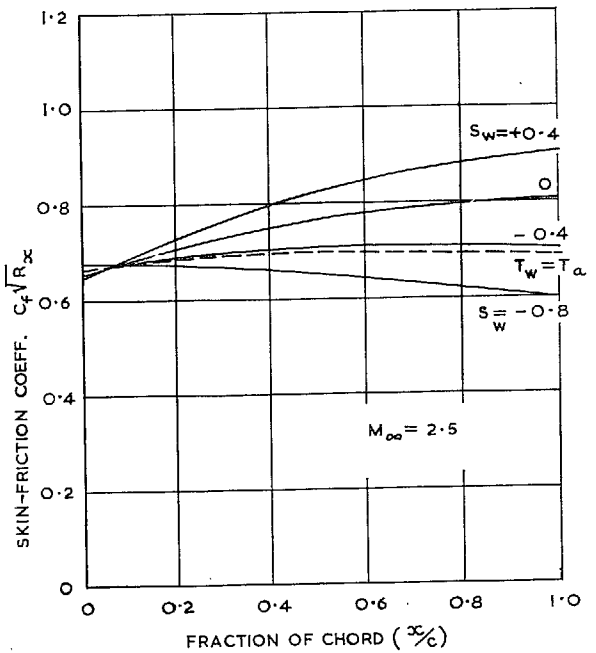

FIG. 3. Effect of wall temperature ratio, 5% thick bi-convex wing section: $M_\infty = 2{\cdot}5$, $x_T/c = 1{\cdot}0$.

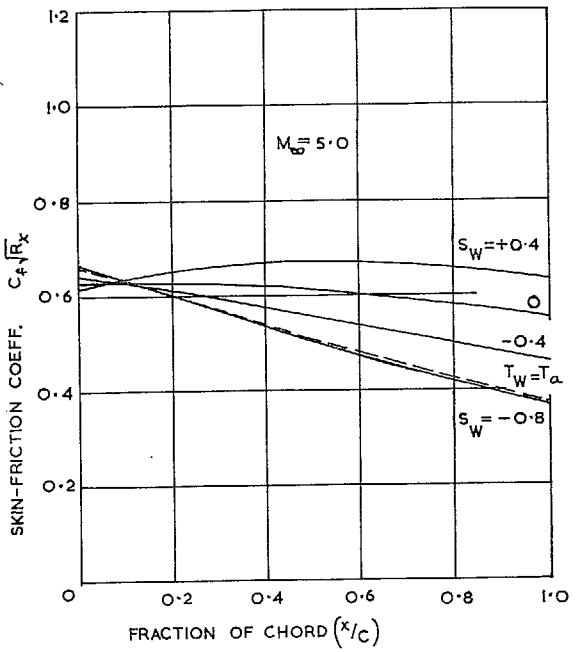

FIG. 4. Effect of wall temperature ratio, 5% thick bi-convex wing section: $M_\infty = 5{\cdot}0$, $x_T/c = 1{\cdot}0$.

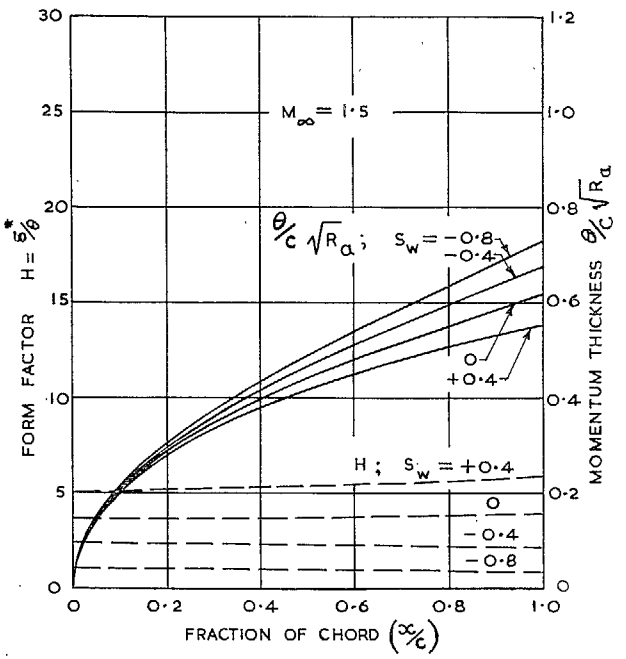

FIG. 5. Effect of wall temperature ratio on H and $(\theta/c)\sqrt{R_a}$; 5% thick bi-convex section: $M_\infty = 1{\cdot}5$, $x_T/c = 1{\cdot}0$.

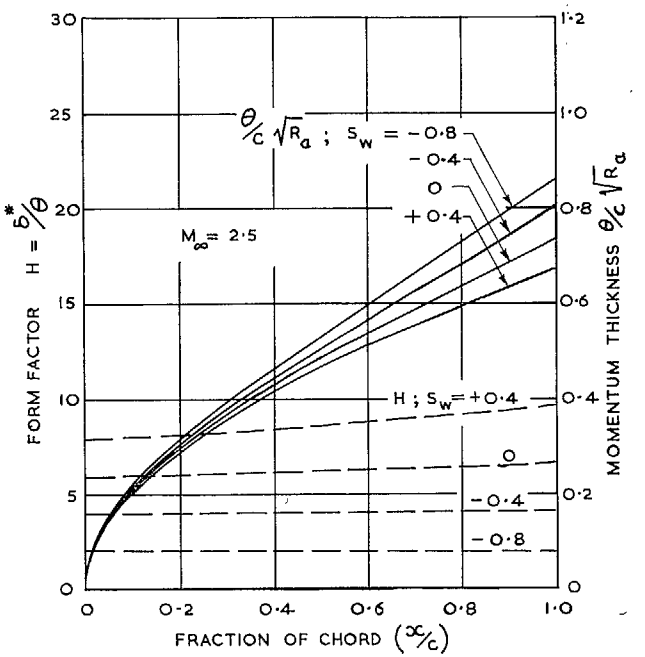

FIG. 6. Effect of wall temperature ratio on H and $(\theta/c)\sqrt{R_a}$; 5% thick bi-convex section: $M_\infty = 2{\cdot}5$, $x_T/c = 1{\cdot}0$.

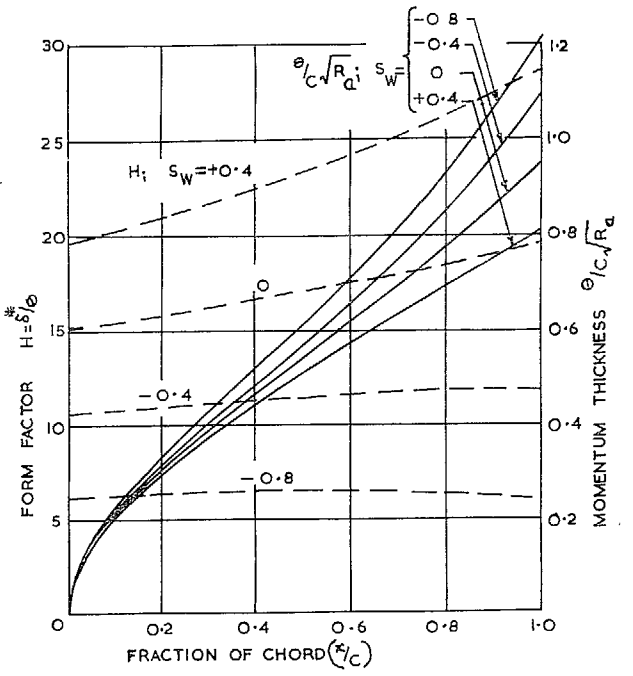

FIG. 7. Effect of wall temperature ratio on H and $(\theta/c)\sqrt{R_a}$; 5% thick bi-convex section: $M_\infty = 5{\cdot}0$, $x_T/c = 1{\cdot}0$.

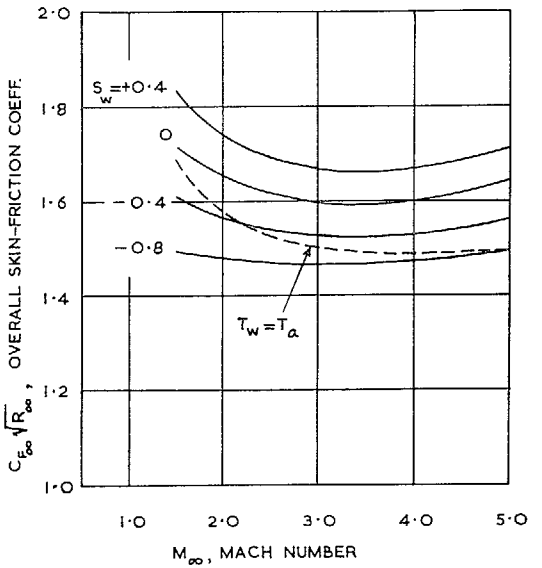

FIG. 8. Influence of Mach number and wall temperature ratio on overall skin-friction coefficient; 5% thick bi-convex wing: $x_T = c$ (one surface).

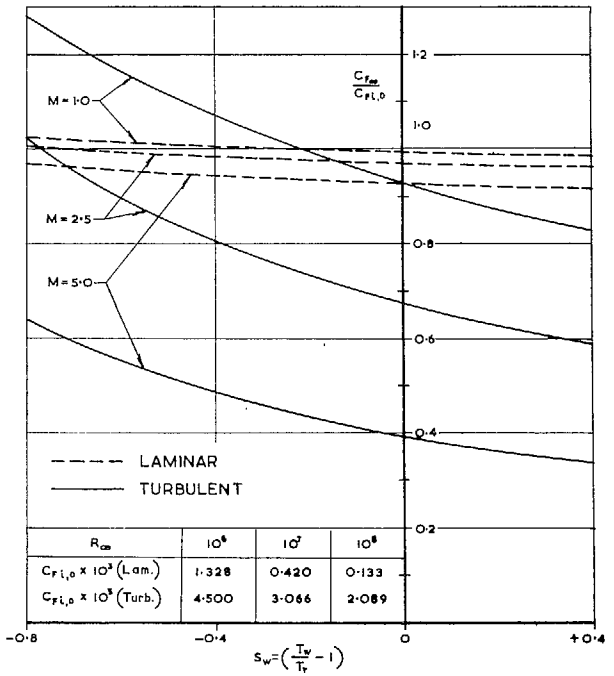

FIG. 9. Skin friction on a flat plate with heat transfer: $\omega = 0{\cdot}89$, $\sigma = 0{\cdot}725$.

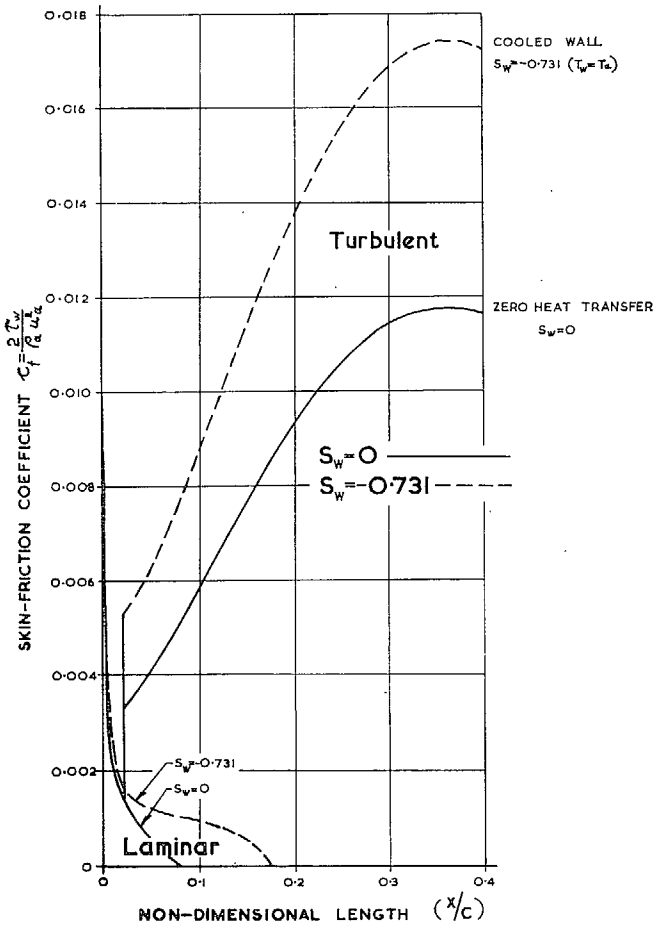

FIG. 10. Effect of heat transfer on skin friction in an adverse pressure gradient: $u_1 = u_\alpha(1-x/c)$, $M_a = 4{\cdot}0$, $\omega = 0{\cdot}89$, $\sigma = 0{\cdot}725$, $x_T/c = 0{\cdot}02$, $R_\infty = 10^7$.

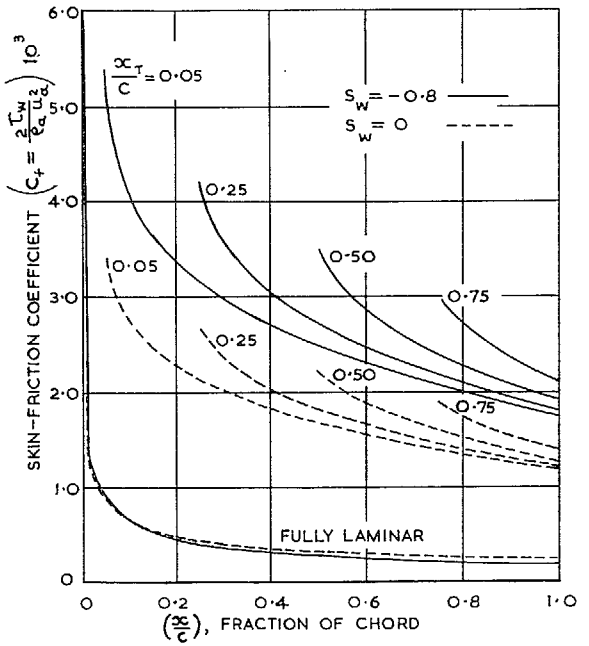

FIG. 11. Influence of cooling on skin-friction distribution; 5% thick bi-convex section: $M_\infty = 2{\cdot}5$, $R_\infty = 10^7$.

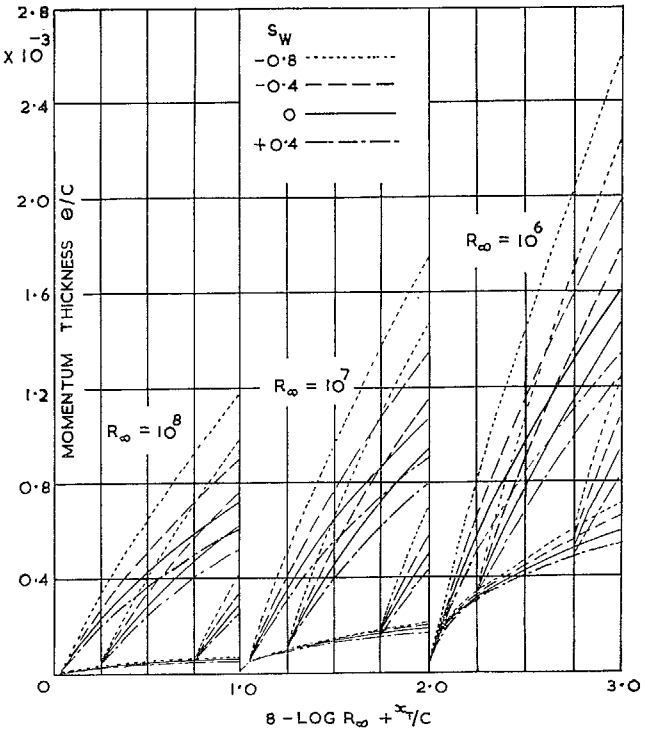

FIG. 12. Momentum thickness on bi-convex wing: $S_w = +0{\cdot}4, 0, -0{\cdot}4, -0{\cdot}8$; $x_T/c = 0{\cdot}05, 0{\cdot}25, 0{\cdot}75, 1{\cdot}00$; $M_\infty = 1{\cdot}5$.

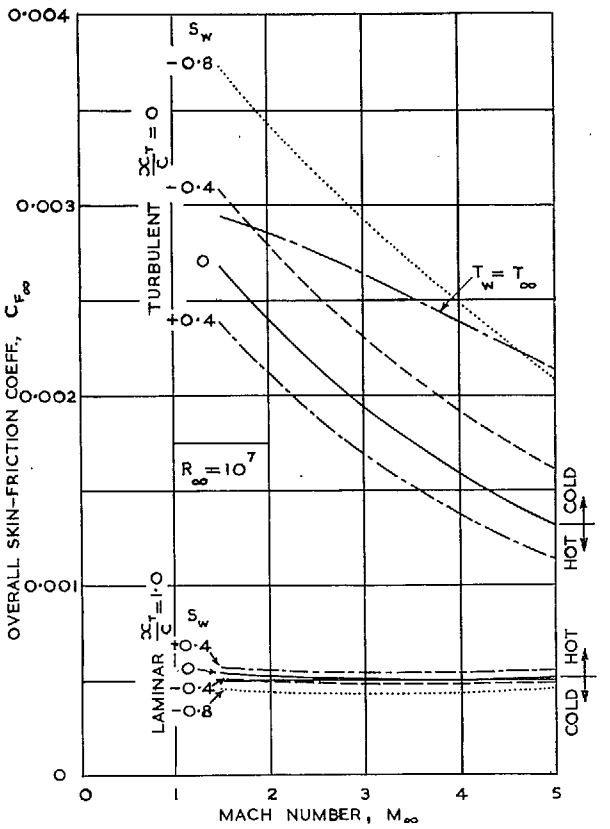

FIG. 13. Skin friction on 5% thick bi-convex wing (one surface).

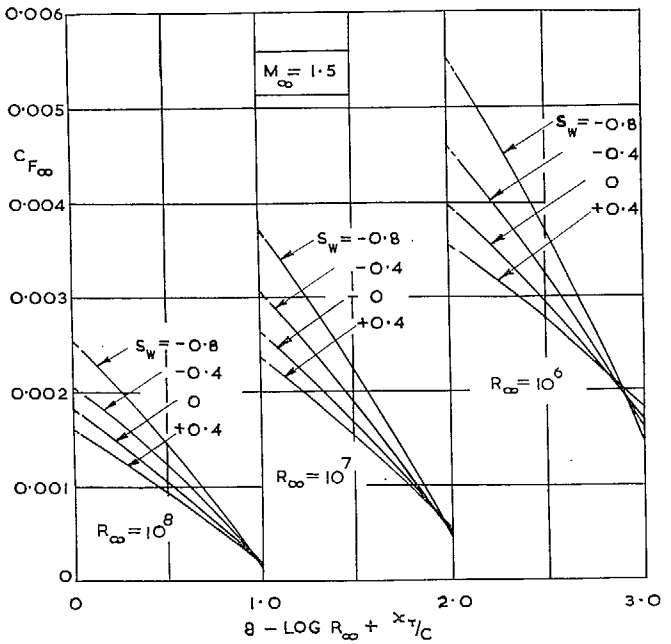

FIG. 14. Skin friction on bi-convex wing (one surface): $t/c = 0·05$, $M_\infty = 1·5$, with heat transfer.

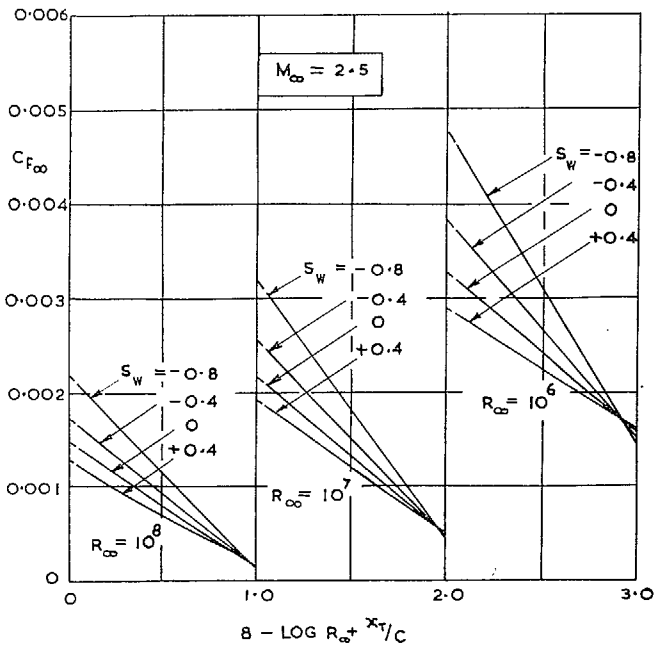

FIG. 15. Skin friction on bi-convex wing (one surface): $t/c = 0·05$, $M_\infty = 2·5$, with heat transfer.

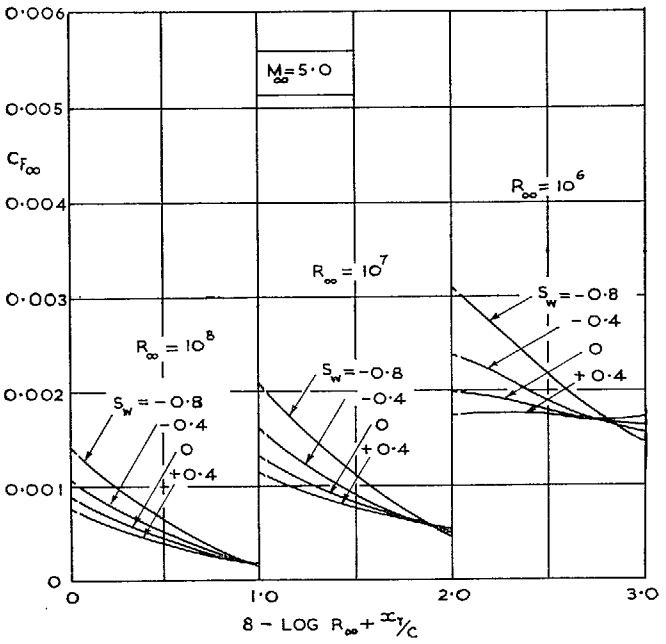

FIG. 16. Skin friction on bi-convex wing (one surface): $t/c = 0·05$, $M_\infty = 5·0$, with heat transfer.

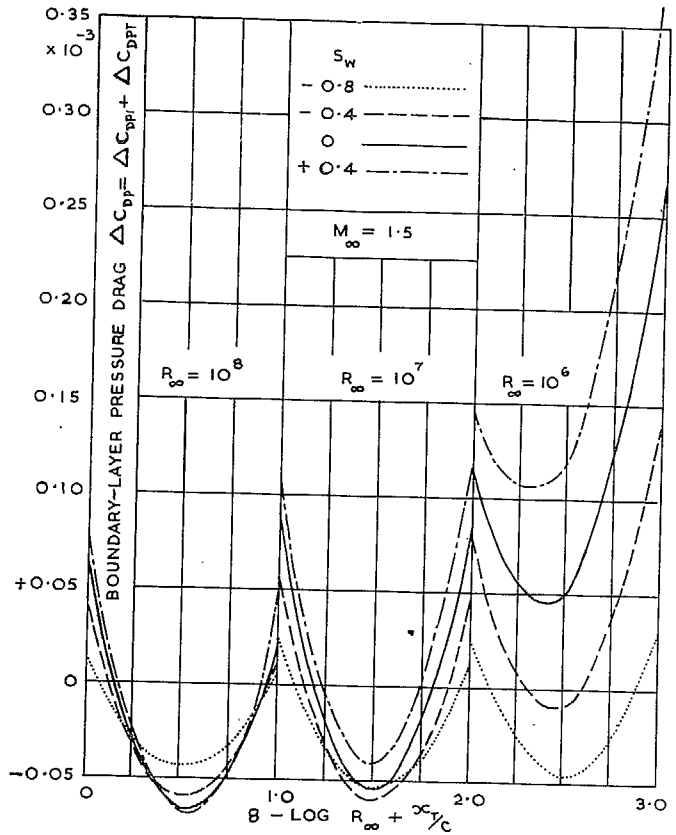

FIG. 17. Boundary-layer pressure drag of 5% thick bi-convex wing (one surface): $M_\infty = 1{\cdot}5$.

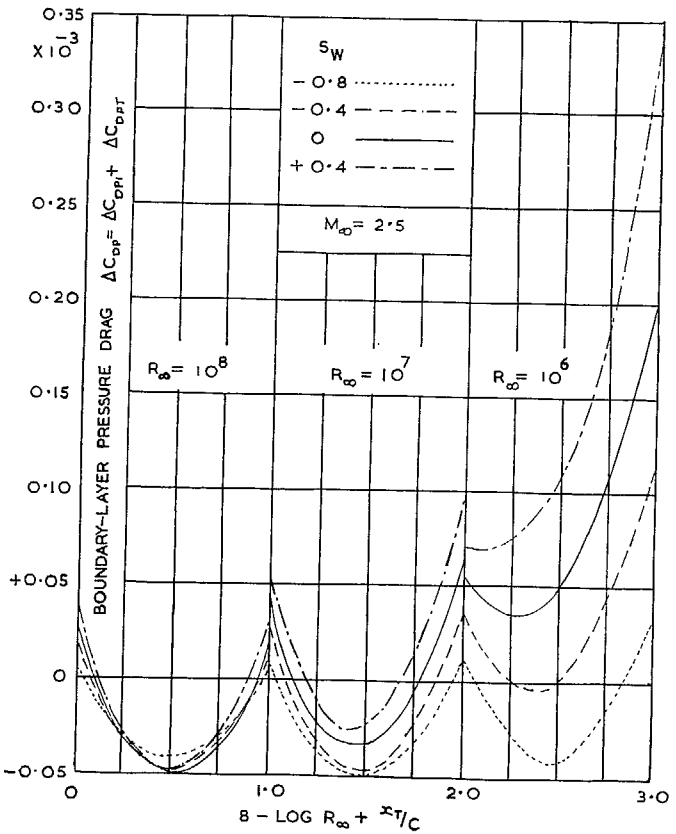

FIG. 18. Boundary-layer pressure drag of 5% thick bi-convex wing (one surface): $M_\infty = 2{\cdot}5$.

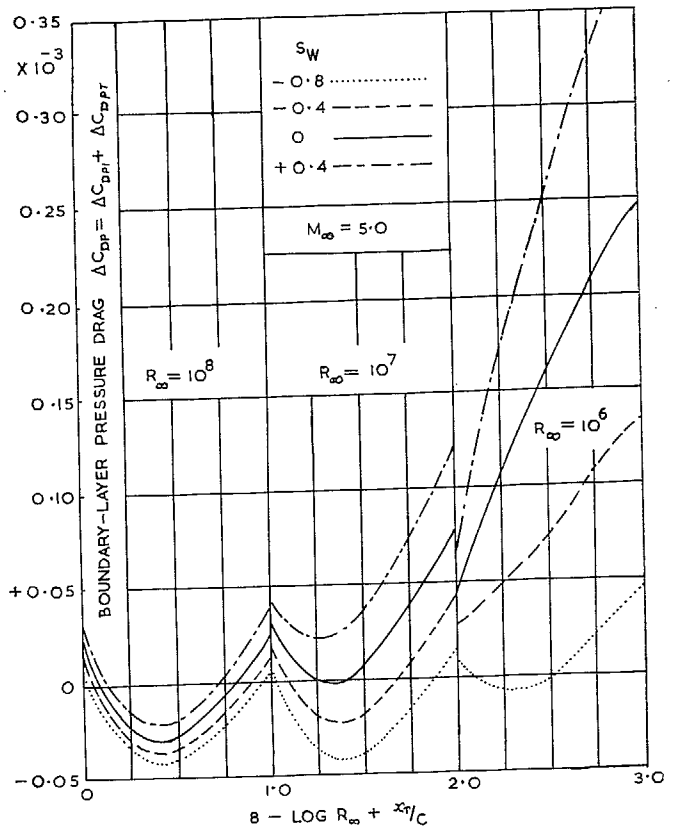

FIG. 19. Boundary-layer pressure drag of 5% thick bi-convex wing (one surface): $M_\infty = 5{\cdot}0$.

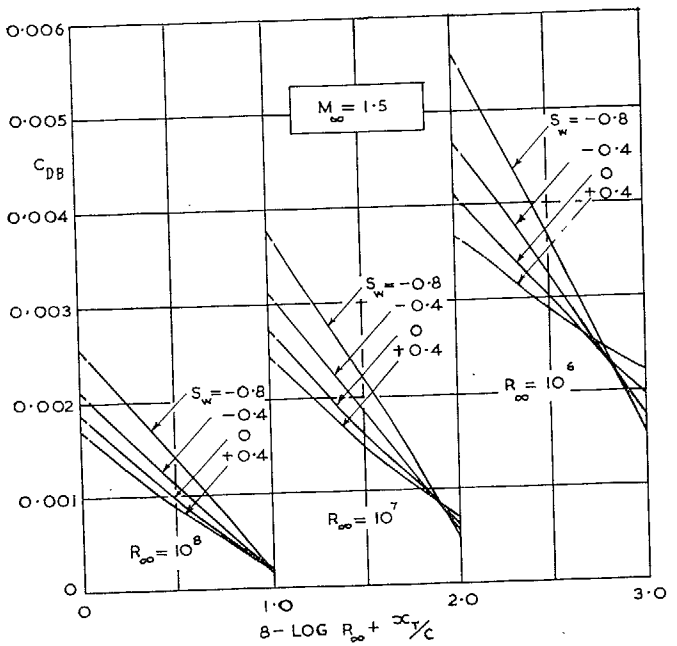

FIG. 20. Boundary-layer drag of 5% thick bi-convex wing (one surface): $M_\infty = 1{\cdot}5$.

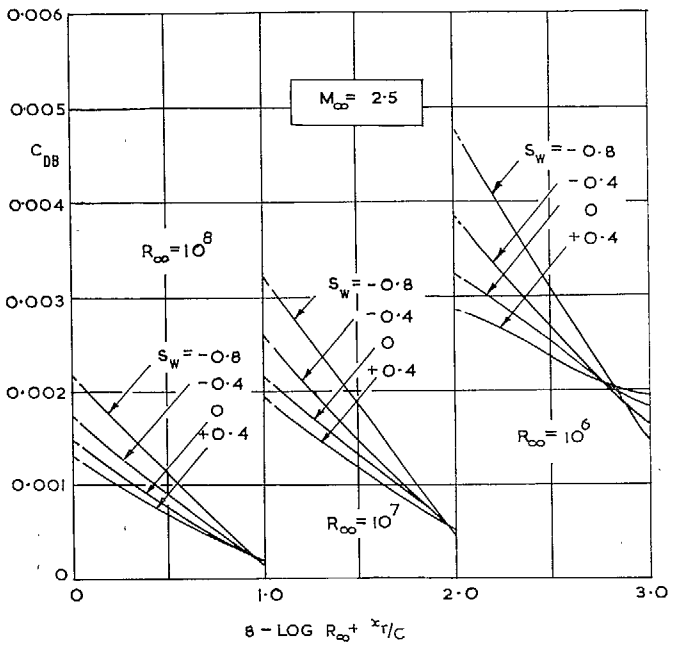

FIG. 21. Boundary-layer drag of 5% thick bi-convex wing (one surface): $M_\infty = 2{\cdot}5$.

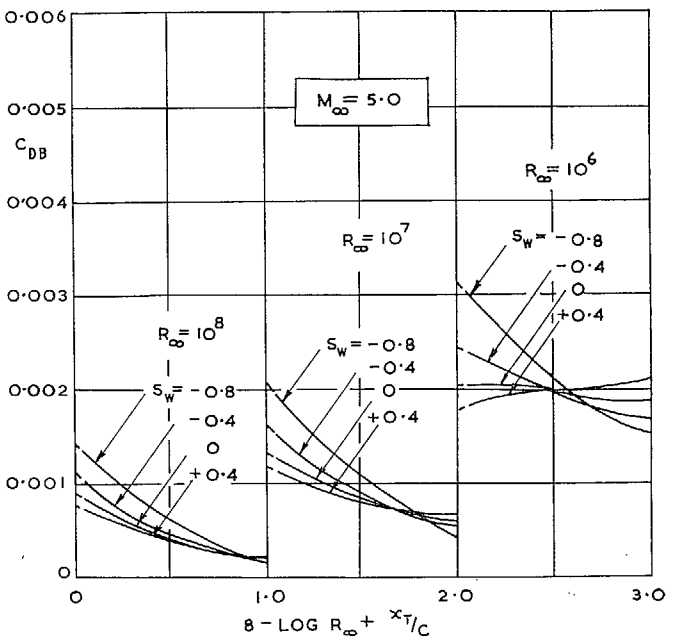

FIG. 22. Boundary-layer drag of 5% thick bi-convex wing (one surface): $M_\infty = 5{\cdot}0$.

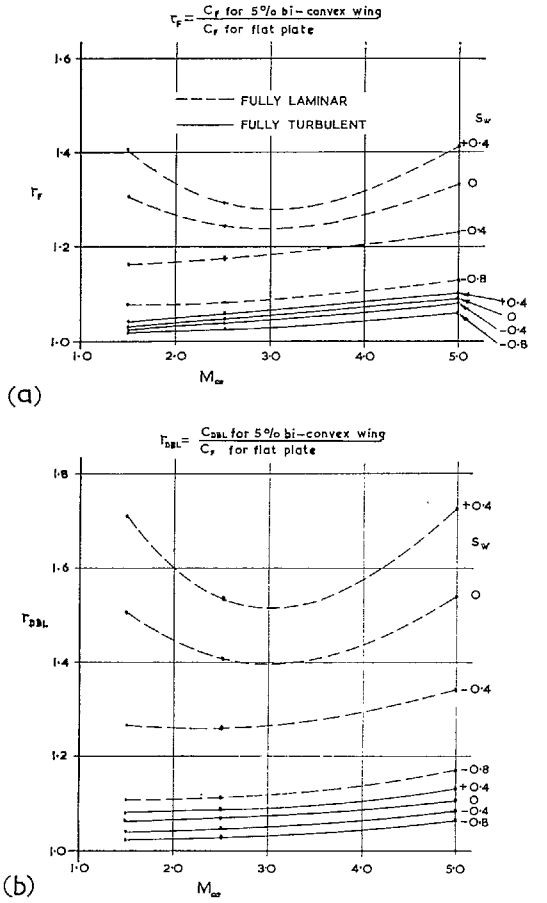

FIG. 23. Effect of wing thickness on (a) skin-friction, (b) boundary-layer drag ($R_\infty = 10^7$).

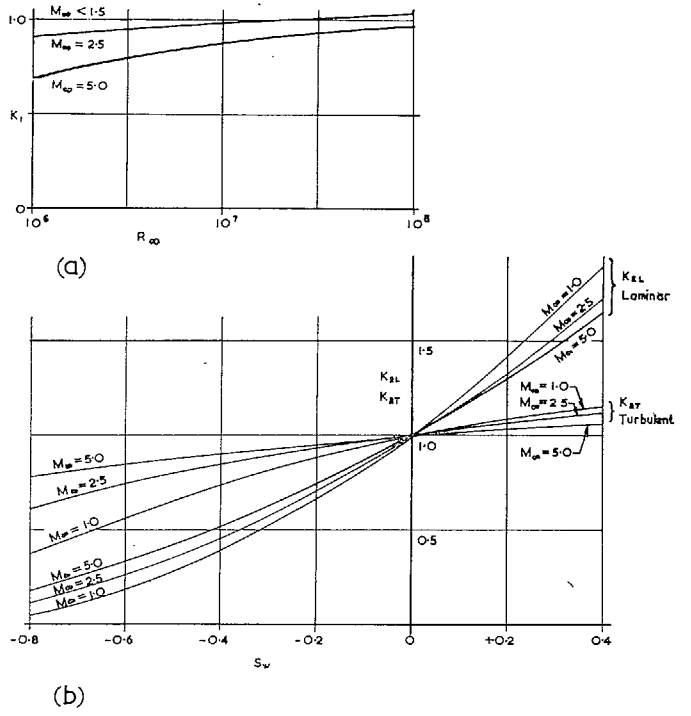

FIG. 24.

(a). Factor K_1, for second-order skin-friction correction for turbulent boundary layer with zero heat transfer allowing for difference between method of Ref. 6 and Spence's method Ref. 2.

(b). Factors for second-order skin-friction correction allowing for effects of heat transfer for laminar boundary layer K_{2L} and turbulent boundary layer K_{2T}.

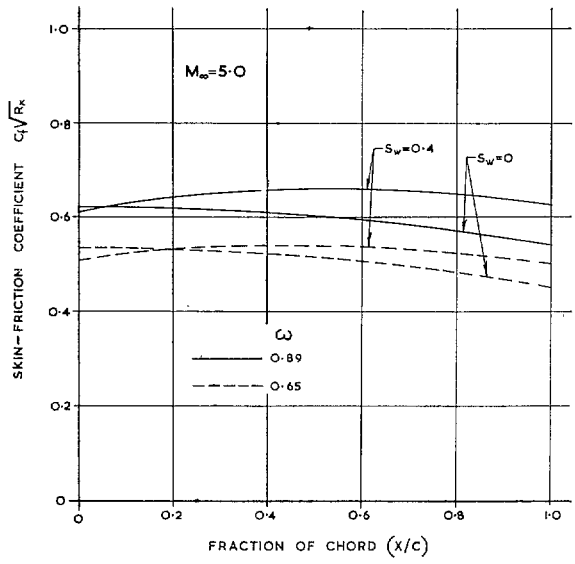

FIG. 25. Influence of ω on skin friction in laminar flow on 5% thick bi-convex section—zero heat transfer and hot-wall cases: $M_\infty = 5{\cdot}0$.

(91261) Wt. 66/2301 K.5 5/65 Hw.

Publications of the Aeronautical Research Council

ANNUAL TECHNICAL REPORTS OF THE AERONAUTICAL RESEARCH COUNCIL (BOUND VOLUMES)

1945 Vol. I. Aero and Hydrodynamics, Aerofoils. £6 10*s*. (£6 13*s*. 6*d*.)
Vol. II. Aircraft, Airscrews, Controls. £6 10*s*. (£6 13*s*. 6*d*.)
Vol. III. Flutter and Vibration, Instruments, Miscellaneous, Parachutes, Plates and Panels, Propulsion. £6 10*s*. (£6 13*s*. 6*d*.)
Vol. IV. Stability, Structures, Wind Tunnels, Wind Tunnel Technique. £6 10*s*. (£6 13*s*. 3*d*.)

1946 Vol. I. Accidents, Aerodynamics, Aerofoils and Hydrofoils. £8 8*s*. (£8 11*s*. 9*d*.)
Vol. II. Airscrews, Cabin Cooling, Chemical Hazards, Controls, Flames, Flutter, Helicopters, Instruments and Instrumentation, Interference, Jets, Miscellaneous, Parachutes. £8 8*s*. (£8 11*s*. 3*d*.)
Vol. III. Performance, Propulsion, Seaplanes, Stability, Structures, Wind Tunnels. £8 8*s*. (£8 11*s*. 6*d*.)

1947 Vol. I. Aerodynamics, Aerofoils, Aircraft. £8 8*s*. (£8 11*s*. 9*d*.)
Vol. II. Airscrews and Rotors, Controls, Flutter, Materials, Miscellaneous, Parachutes, Propulsion, Seaplanes, Stability, Structures, Take-off and Landing. £8 8*s*. (£8 11*s*. 9*d*.)

1948 Vol. I. Aerodynamics, Aerofoils, Aircraft, Airscrews, Controls, Flutter and Vibration, Helicopters, Instruments, Propulsion, Seaplane, Stability, Structures, Wind Tunnels. £6 10*s*. (£6 13*s*. 3*d*.)
Vol. II. Aerodynamics, Aerofoils, Aircraft, Airscrews, Controls, Flutter and Vibration, Helicopters, Instruments, Propulsion, Seaplane, Stability, Structures, Wind Tunnels. £5 10*s*. (£5 13*s*. 3*d*.)

1949 Vol. I. Aerodynamics, Aerofoils. £5 10*s*. (£5 13*s*. 3*d*.)
Vol. II. Aircraft, Controls, Flutter and Vibration, Helicopters, Instruments, Materials, Seaplanes, Structures, Wind Tunnels. £5 10*s*. (£5 13*s*.)

1950 Vol. I. Aerodynamics, Aerofoils, Aircraft. £5 12*s*. 6*d*. (£5 16*s*.)
Vol. II. Apparatus, Flutter and Vibration, Meteorology, Panels, Performance, Rotorcraft, Seaplanes. £4 (£4 3*s*.)
Vol. III. Stability and Control, Structures, Thermodynamics, Visual Aids, Wind Tunnels. £4 (£4 2*s*. 9*d*.)

1951 Vol. I. Aerodynamics, Aerofoils. £6 10*s*. (£6 13*s*. 3*d*.)
Vol. II. Compressors and Turbines, Flutter, Instruments, Mathematics, Ropes, Rotorcraft, Stability and Control, Structures, Wind Tunnels. £5 10*s*. (£5 13*s*. 3*d*.)

1952 Vol. I. Aerodynamics, Aerofoils. £8 8*s*. (£8 11*s*. 3*d*.)
Vol. II. Aircraft, Bodies, Compressors, Controls, Equipment, Flutter and Oscillation, Rotorcraft, Seaplanes, Structures. £5 10*s*. (£5 13*s*.)

1953 Vol. I. Aerodynamics, Aerofoils and Wings, Aircraft, Compressors and Turbines, Controls. £6 (£6 3*s*. 3*d*.)
Vol. II. Flutter and Oscillation, Gusts, Helicopters, Performance, Seaplanes, Stability, Structures, Thermodynamics, Turbulence. £5 5*s*. (£5 8*s*. 3*d*.)

1954 Aero and Hydrodynamics, Aerofoils, Arrester gear, Compressors and Turbines, Flutter, Materials, Performance, Rotorcraft, Stability and Control, Structures. £7 7*s*. (£7 10*s*. 6*d*.)

Special Volumes

Vol. I. Aero and Hydrodynamics, Aerofoils, Controls, Flutter, Kites, Parachutes, Performance, Propulsion, Stability. £6 6*s*. (£6 9*s*.)
Vol. II. Aero and Hydrodynamics, Aerofoils, Airscrews, Controls, Flutter, Materials, Miscellaneous, Parachutes, Propulsion, Stability, Structures. £7 7*s*. (£7 10*s*.)
Vol. III. Aero and Hydrodynamics, Aerofoils, Airscrews, Controls, Flutter, Kites, Miscellaneous, Parachutes, Propulsion, Seaplanes, Stability, Structures, Test Equipment. £9 9*s*. (£9 12*s*. 9*d*.)

Reviews of the Aeronautical Research Council

1949–54 5*s*. (5*s*. 5*d*.)

Index to all Reports and Memoranda published in the Annual Technical Reports

1909–1947 R. & M. 2600 (out of print)

Indexes to the Reports and Memoranda of the Aeronautical Research Council

Between Nos. 2451–2549: R. & M. No. 2550 2*s*. 6*d*. (2*s*. 9*d*.); Between Nos. 2651–2749: R. & M. No. 2750 2*s*. 6*d*. (2*s*. 9*d*.); Between Nos. 2751–2849: R. & M. No. 2850 2*s*. 6*d*. (2*s*. 9*d*.); Between Nos. 2851–2949: R. & M. No. 2950 3*s*. (3*s*. 3*d*.); Between Nos. 2951–3049: R. & M. No. 3050 3*s*. 6*d*. (3*s*. 9*d*.); Between Nos. 3051–3149: R. & M. No. 3150 3*s*. 6*d*. (3*s*. 9*d*.); Between Nos. 3151–3249: R. & M. No. 3250 3*s*. 6*d*. (3*s*. 9*d*.); Between Nos. 3251–3349: R. & M. No. 3350 3*s*. 6*d*. (3*s*. 10*d*.)

Prices in brackets include postage

Government publications can be purchased over the counter or by post from the Government Bookshops in London, Edinburgh, Cardiff, Belfast, Manchester, Birmingham and Bristol, or through any bookseller

Printed and published by
HER MAJESTY'S STATIONERY OFFICE

To be purchased from
York House, Kingsway, London W.C.2
423 Oxford Street, London W.1
13A Castle Street, Edinburgh 2
109 St. Mary Street, Cardiff
39 King Street, Manchester 2
50 Fairfax Street, Bristol 1
35 Smallbrook, Ringway, Birmingham 5
80 Chichester Street, Belfast 1
or through any bookseller

Printed in England

R. & M. No. 3393

S.O. Code No. 33-3393